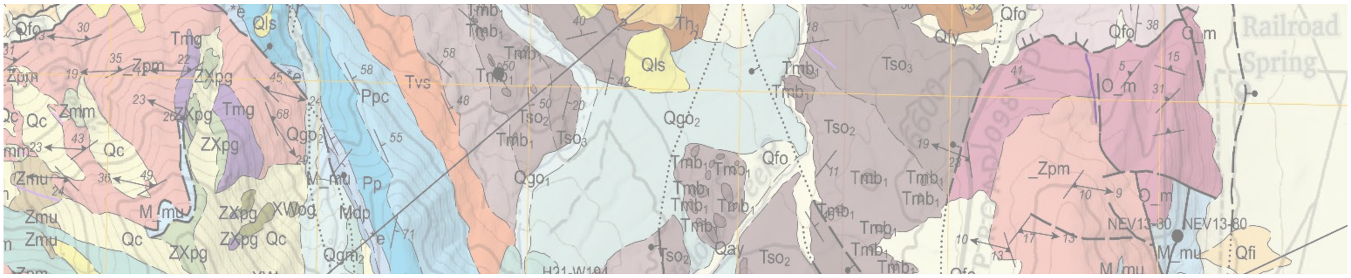

TEXT AND REFERENCES ACCOMPANYING NEVADA BUREAU OF MINES AND GEOLOGY OPEN-FILE REPORT 2025-08

Geologic Map of the Ruby Mountains–East Humboldt Range–Wood Hills–Pequop Mountains Metamorphic Core Complex Region, Elko County, Nevada

by

Andrew V. Zuza, Seth Dee, and Christopher D. Henry

Nevada Bureau of Mines and Geology, University of Nevada, Reno

2025

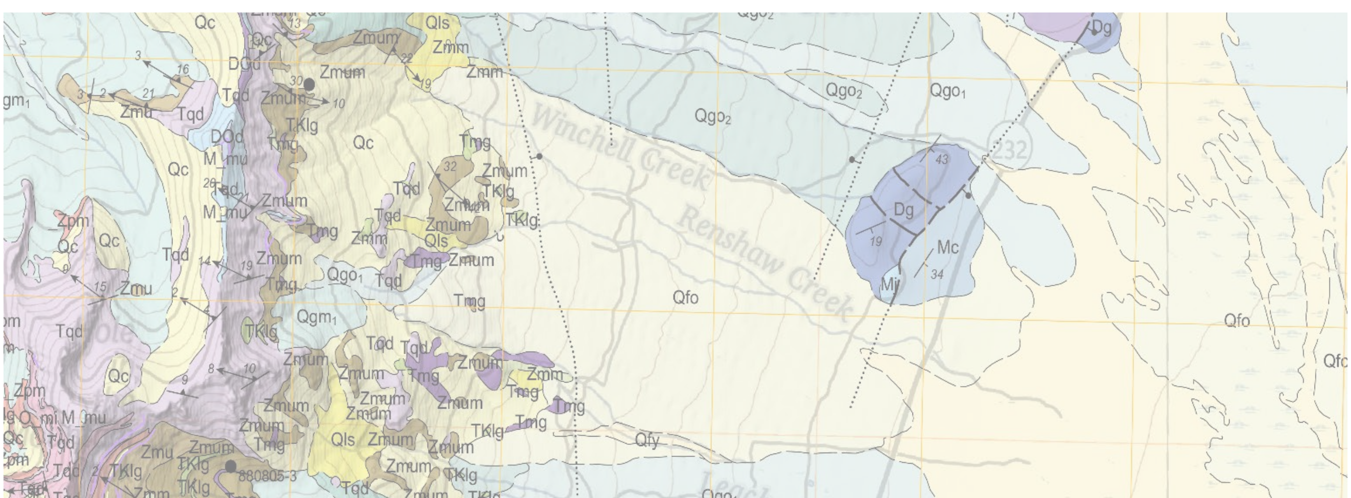

Suggested citation:
Zuza, A.V., Dee, S., and Henry, C.D., 2025, Geologic map of the Ruby Mountains–East Humboldt Range–Wood Hills–Pequop Mountains metamorphic core complex region, Elko County, Nevada: Nevada Bureau of Mines and Geology Open-File Report 2025-08, scale 1:62,500, 29 p.

NBMG open-file reports have not undergone formal peer review. This geologic map was funded in part by the USGS National Cooperative Geologic Mapping Program under the STATEMAP award numbers G21AC10873, 2021 and G22AC00578, 2022, and with support from the Geological Society of Nevada.

ABSTRACT

This 1:62,500-scale geologic map encompasses much of the Ruby Mountains–East Humboldt Range–Wood Hills–Pequop Mountains (REWP) metamorphic core complex (MCC) in Elko County, northeast Nevada. The map area covers the northernmost Ruby Mountains, most of the East Humboldt Range, the Wood Hills, the northern Pequop Mountains, and adjacent valleys (e.g., from west to east, Starr Valley, Secret Valley, Clover Valley, Independence Valley, and Goshute Valley). This compilation map reveals important field relationships that bracket the Mesozoic–Cenozoic evolution of the REWP MCC, associated with Mesozoic contractional deformation and crustal thickening and followed by Cenozoic metamorphic core complex formation and extension. Bedrock units consist of Archean(?)–Proterozoic para- and orthogneiss, Neoproterozoic–Triassic passive margin stratigraphy, and Mesozoic–Cenozoic intrusions and volcanic rocks. The pre-Cenozoic stratigraphy is variably metamorphosed, with higher metamorphic grade rocks found in the west in the core of the REWP MCC; upper greenschist-lower amphibolite grade rocks are exposed in the Ruby Mountains–East Humboldt Range, whereas unmetamorphosed upper Paleozoic strata are observed in the Pequop Mountains. Mesozoic contractional deformation is best evidenced by the southeast-directed Independence thrust fault in the Pequop Mountains, which is interpreted to have been active in the Late Jurassic based on a crosscutting Late Jurassic lamprophyre sill. Other possible Mesozoic contractional deformation includes observed older-over-young fault relationships within the East Humboldt Range and complex fold nappes observed within the core of the REWP MCC. Scattered Late Jurassic intrusions are observed across the study area. Late Cretaceous intrusions are predominately peraluminous granites associated with voluminous crustal melting that are very common in the core of the REWP, but they are also found in the Wood Hills and Pequop Mountains as minor dikes. In the Cenozoic, relatively primitive Eocene quartz diorite and gabbro sills intruded the Ruby Mountains–East Humboldt Range, which greatly heated the mid-crust and was followed by the emplacement of more evolved Oligocene monzogranite bodies. A ~1 km thick mylonitic shear zone that deformed Oligocene and older rocks along the western flank of the East Humboldt Range but is crosscut by ca. 17 Ma basalt dikes led to the domal exhumation of the core of REWP MCC. We interpret that this Oligocene doming was driven by heating and melting of the lower-plate rocks, as evidenced by the spatial correspondence of Oligocene plutonism and REWP MCC shear zones. This exhumation did not generate any observed syn-kinematic sediments. A smaller subdome may have developed beneath the Wood Hills to generate the ~1.5 km wavelength recumbent folds within the Wood Hills.

Later, Miocene regional extension first generated a series of apparent low-angle normal faults followed by high-angle normal faults. The apparently low-angle normal faults are subparallel to bedding, such as the Pequop fault or the Ruby Mountains–East Humboldt Range detachment fault, but these faults reactivated existing inclined structures, including the hanging wall of the Independence thrust in the Pequop Mountains and the margins of the domal REWP MCC in the East Humboldt Range, respectively. Therefore, these early normal faults actually initiated at moderate dips (40–50°) and tilted the major mountain ranges in their footwalls. In the East Humboldt Range, the detachment fault cuts ca. 17 Ma basalt dikes, which implies activity in the middle Miocene. Miocene extension led to the formation of the syn-kinematic sequence of Clover Creek and Humboldt Formation, which are observed across the compilation area. Later high-angle normal faulting has continued to impact the study area, including active fault scarps observed along the western flanks of the East Humboldt Range and Pequop Mountains.

The Quaternary deposits in the compilation map area record two major glaciations, late Pleistocene Lake Clover, and active normal faulting. In the Ruby Mountains–East Humboldt Range, glacial deposits associated with the Angel Lake and Lamoille glaciations are well preserved. Fault scarps cut glacial outwash surfaces associated with these glaciations, with 7 m and 30 m scarps respectively, yielding vertical separation rates of ~0.21–0.35 mm/yr in the latest Pleistocene and ~0.09–0.17 mm/yr in the late Pleistocene. The normal faults that bound the western flank of the Pequop Mountains likely involved similar slip rates. In the Independence and Goshute valleys lacustrine gravels are deposited on shorelines, beach bars, and spits recording the highstand and recessional stages of latest Pleistocene Lake Clover.

DESCRIPTION OF MAP UNITS

Quaternary Deposits

Water Perennial water bodies including Snow Water Lake in Clover Valley and small ponds in Independence Valley.

Hillslope Deposits

Qc Colluvium (Holocene) Unconsolidated, angular to slightly rounded boulders to pebbles of bedrock in a variably sandy and silty matrix. At and near the range front, material is cobble-dominated with ~30% matrix. The upper reaches of catchments affected by late Pleistocene glaciation have slopes with very coarse matrix-free talus. Commonly 1–5 m thick.

Qls Landslide deposits (Holocene to late Pleistocene) Minor slope failure deposits with a wide range of characteristics and compositions. Locally dominated by highly fractured or jumbled bedrock, with a varying percentage of poorly to moderately sorted gravels and fines. Typically form uneven, hummocky surfaces. Head scarps vary from sharp and fresh to rounded and indistinct.

Qmls Mega-landslide deposits (middle Pleistocene?) Undivided mega-landslide deposits with intermixed, blocks of bedrock that forms uneven hummocky surfaces. On the west flank of Tent Mountain, a Qmls deposit includes blocks of quartzite, leucogranite, monzogranite, and marble up to 10 m long. Another Qmls deposit located between Reed and Heelfly creeks contains fractured blocks of rhyolite, basalt and tuffaceous sedimentary rocks up to 100 m long. Fault scarps are locally present in both deposits.

Groundwater Discharge, Eolian, and Playa Deposits

Qgwd Groundwater discharge deposits (Holocene to Pleistocene) Organic-rich fine silt and clay around and down slope from active springs. Dominated by eolian material trapped by vegetation associated with spring discharge, but may include material transported by surface water. The deposits are variably calcareous and locally weakly stratified. Along the western range front of the East Humboldt Range, Qgwd deposits are common at active springs overlying faults with late-Quaternary activity. Deposits are generally less than 2 m thick.

Qpa Playa and alluvial deposits (Holocene) Fine-grained deposit in the nearly flat axis of Independence and Clover valleys; typically light gray to grayish brown silt, clay, and minor fine sand. Deposited during inundation of the playa with shallow standing water. Sediments include evaporite deposits and efflorescent salt crusts. Interfingers with, and locally overlain by, Qgwd deposits in Independence Valley.

Qe Eolian sand (Holocene) Light brown, well-sorted, fine- to medium-grained sand deposits in Independence and Goshute valleys. Commonly forms barchan dunes with asymmetries suggesting prevailing winds out of the east-northeast. Deposits are generally less than 2 m thick.

Lacustrine Deposits

Qla Lacustrine and alluvial deposits (Holocene to late Pleistocene) Variable deposits of lacustrine silt, clay, and sand; and alluvial silt, sand, and minor gravel. Lacustrine silt was deposited in shallow waters of late Pleistocene lakes. Lake Clover, which occupied the Clover and Independence valleys, had highstands at approximately 19.5 ka and 17.0 ka (Munroe and Laabs, 2013). Lake Warring in Goshute Valley had a highstand at 16.8 ka (Munroe and Laabs, 2013). Alluvial deposits are present in channels and are comprised of reworked lacustrine deposits and distal fan sediments.

Qlg Lacustrine gravels (late Pleistocene) Gray to brown deposits of moderately to well-sorted pebble- to cobble-sized gravel and sand in shorelines, beach bars, and spits. Clasts are rounded to subrounded. Soils consist of 20- to 30-cm-thick Bw horizon, underlain by 30–50 cm stage II $CaCO_3$ horizons (Bk). Snail shells are common. Unit was deposited during highstands and regressive phases of late Pleistocene Lake Clover and Lake Warring. Lake Clover reached a maximum elevation of 1,729 m at 19.5 ka and 17.0 ka (Munroe and Laabs, 2013). Lake Waring reached a maximum late Pleistocene elevation of 1,761 m (Reheis, 1999) at 16.8 ka (Munroe and Laabs, 2013). Qlg shoreline deposits are inset into Qfi fan deposits. Exposed thickness of unit is 3+ m.

Alluvial Deposits

Qra_1 Active floodplain alluvium (late Holocene) Deposits of well-sorted clay, silt, and sand within the active floodplain and major channels of the Humboldt and Marys rivers. Includes seasonally inundated terrace surfaces, meander belts, sloughs and overflow channels.

Qay Young alluvium (Holocene) Deposits of mud, silt, sand, and pebble- to cobble-sized gravel in active and ephemeral channels and floodplains.

Qfy Young alluvial-fan deposits, undivided (Holocene) Deposits of silt, sand and pebble- to cobble- sized gravel in active and recently abandoned alluvial fans and ephemeral stream channels. Includes subrounded to subangular clasts of bedrock derived from the adjacent mountain ranges. Alluvial fan surfaces vary from having pronounced bar-and-swale morphology near fan heads and within active channels to generally smooth and mildly dissected by gully erosion at mid- and distal-fan locations. Commonly inset topographically below adjacent older deposits. Includes undivided Qfy_2 deposits.

Qra_2 Recently abandoned floodplain alluvium (middle to early Holocene) Deposits of well-sorted clay, silt and sand, and rare gravels within recently abandoned floodplain terraces of the Humboldt and Marys rivers. Includes abandoned terrace surfaces and meander belts with 1 to 3 m of topographic separation from Qra_1. May be inundated during infrequent flooding.

Qfy_2 Young alluvial-fan deposits (middle to early Holocene) Deposits of silt, sand and pebble- to cobble-sized gravel with local boulders in generally inactive alluvial fans. Includes subrounded to subangular clasts of bedrock derived from the adjacent mountain ranges. Surfaces are generally smooth and mildly dissected by gully incision. Qfy_2 is only distinguished from the undivided Qfy map unit along the western piedmont of the East Humboldt Range, where it has been uplifted 1–2.5 m in the footwall of the Ruby Mountains fault zone fault by the most recent surface-rupturing earthquake Carbon obtained from the unit in a paleoseismic trench at Reed Creek yielded a 14C radiocarbon age of 7,500 + 70 cal yr B.P (Wesnousky and Willoughby, 2003)..

Qra_3 Abandoned floodplain alluvium (late Pleistocene) Deposits of well-sorted silt, sand, and gravels within abandoned terraces of the Humboldt and Marys rivers. Includes rounded to subrounded clasts of mylonitic quartzite, gneiss, rhyolite, basalt, welded tuff and granitic rocks derived from a large regional catchment. Commonly buried by 0.5–1 m of eolian silt. The Qra_3 terrace forms several extensive flat surfaces that are 6 to 9 m above the active floodplain.

Qra_4 Older floodplain alluvium (late Pleistocene?) Deposits of well-sorted silt, sand, and gravels within abandoned terraces of the Humboldt River. Includes rounded to subrounded clasts of mylonitic quartzite, gneiss, rhyolite, basalt, welded tuff, and granitic rocks. Qra_4 is preserved in isolated terrace remnants that are 13 to 16 m above the active floodplain.

Qai Intermediate-age alluvium (late Pleistocene) Deposits of silt, sand, and pebble- to cobble-sized gravel with boulders. Includes rounded to sub rounded clasts of mylonitic quartzite, gneiss, and granitic rocks. Preserved as terrace surfaces inset into older alluvial deposits along Soldier Creek, Secret Creek, Stephens Creek, and tributaries. Terrace surfaces are smooth, locally dissected, broadly rounded and topographically 3–15 m above active floodplains. Approximately age correlative with glacial outwash deposits associated with latest Pleistocene Angel Lake glaciation (Qgo_1).

Qfi Intermediate-age alluvial-fan deposits (late Pleistocene) Deposits of silt, sand, and pebble- to cobble-sized gravel with boulders. Includes subrounded to subangular clasts of bedrock derived from the adjacent mountain ranges. Surfaces are planar, dissected, and topographically separated from Qfy deposits. Absent at the mouths of glaciated drainages suggesting Qfi may be time correlative with glacial outwash deposits associated with latest Pleistocene Angel Lake glaciation (Qgo_1).

Qfo Older alluvial-fan deposits, undivided (middle Pleistocene?) Coarse-grained alluvial deposits in inactive alluvial fans; typically sandy pebble- to cobble-sized gravel with boulders. Clasts are subrounded to subangular bedrock derived from the adjacent mountain ranges. Surface morphology ranges from planar to fully rounded erosional remnants. Locally mantled by an eolian cap. Surfaces without a significant eolian accumulation have abundant litter of pedogenic carbonate. Surfaces are highly dissected with incised channels up to 20 m deep. Upper soil horizons are erosionally stripped, Stage III–IV $CaCO_3$ horizons up to 2.5 m thick commonly form a continuous carbonate-rich layer with local development of laminar carbonate structure. Exposed thickness of the unit is 5 m to ~20 m.

Qfo_1, Qfo_2, Qfo_3, and Qfo_4 Older alluvial-fan deposits (middle Pleistocene?) Four distinct and topographically correlative terrace and pediment surfaces (Qfo_1, Qfo_2, Qfo_3, and Qfo_4) are preserved on the uplifted footwall of the Ruby Mountains fault along the west side of the East Humboldt Range. Unit descriptions the same as the undivided Qfo map unit. South of Herder Creek, divided Qfo surfaces are beveled onto Tertiary sediments, and to the north, they are preserved as small remnants deposited on crystalline bedrock. Qfo_3 is a regionally extensive surface that Sharp (1940) named the "Lee" surface.

QTf Oldest alluvial-fan deposits (middle Pleistocene? to Pliocene?) Coarse-grained alluvial deposits; typically sandy pebble- to cobble-sized gravel with abundant boulders. Clasts are subrounded to subangular bedrock derived from the adjacent mountain ranges. Surfaces are fully rounded erosional remnants and soil horizons are entirely stripped. Maximum exposed thickness of the unit is approximately 20 m.

QTa Oldest alluvium (middle Pleistocene? to Pliocene?) Deposits of silt, sand, and pebble gravel. Poorly exposed in the basin west of the Ruby Mountains–East Humboldt range front. QTa deposits are gullied and eroded with no preservation of original geomorphic surfaces or overlying soils. Locally overlain by Qfo alluvial-fan deposits. QTa is likely distal alluvial deposits sourced from the Ruby Mountains–East Humboldt Range with fine-grained lacustrine interbeds. Clasts are subangular to subrounded mylonitic quartzite and gneiss. A 2.35±0.7 Ma vitric ash bed (Qva) is present in the lower part of the exposed QTa deposit along the western margin of the map area, with sufficient exposed thickness beneath the ash to suggest the lower part of the section may be Pliocene in age. Correlative with fluvio-lacustrine sediments deposited in and around a shallow lake covering much of the Elko basin during a temporary blockage of Humboldt River, beginning possibly during the Pliocene and continuing into the Pleistocene (Wallace et al., 2008). Exposed thickness is ~60 m.

Glacial and Related Deposits

Qgo_1 Glacial outwash deposits, Angel Lake age (late Pleistocene) Deposits of silt, sand, and pebble- to cobble-sized gravel with boulders up to 3 m in diameter. Includes rounded to subrounded clasts of mylonitic quartzite, gneiss, and granitic rocks. Alluvial outwash from the Angel Lake glacial advance.

Cosmogenic 10Be exposure ages of boulders atop Qgo_1 surface at the mouth of Greys Creek adjacent to the East Humboldt Range have two groupings of ages (Zuza et al., 2021a). A grouping of three boulders with exposure ages ranging from 27–14 ka, which corresponds with previously published ages from glacial deposits of the last glaciation in the Ruby Mountains–East Humboldt Range (Laabs et al., 2020). This is the preferred age for the Qgo_1 geomorphic surface and suggests that the outwash surface is correlated to the Angel Lake glaciation (as termed by Sharp, 1938). Another grouping of three boulders with ages ranging from 81–65 ka suggest a period of aggradation that may be associated with glaciation that is not well preserved in the moraine record.

Qgm Glacial moraine deposits, undivided, Angel Lake and Lamoille age (late to middle Pleistocene) Deposits of poorly sorted sand, gravel, and boulders up to 6 m in diameter. Includes subangular to subrounded clasts of mylonitic quartzite, gneiss and granitic rocks. Moraine deposits include lateral and medial moraines, as well as subglacial and ablation till. Moraine crests commonly have sharp morphology, but are locally rounded and subdued. Most undivided Qgm deposits in the map area are likely from the late Pleistocene Angel Lake glaciation, in areas where a clear distinction between younger and older moraines was not identified, and therefore, deposits from the older Lamoille glaciation are presumed to be locally present (Sharp, 1938; Laabs et al., 2020).

Qgm_1 Glacial moraine deposits, Angel Lake age (late Pleistocene) Deposits of poorly sorted sand, gravel, and boulders up to 6 m in diameter forming lateral moraines from the Angel Lake glacial advance, moraine crests shown. Includes subangular to subrounded clasts of mylonitic quartzite, gneiss and granitic rocks. Moraine crests are sharp with abundant boulders. Locally inset adjacent to Lamoille age moraines.

Qgo_2 Glacial outwash deposits, Lamoille age (middle Pleistocene) Deposits of silt, sand, and pebble-cobble gravel with boulders up to 6 m in diameter. Includes rounded to subrounded clasts of mylonitic quartzite, gneiss and granitic rocks. Alluvial outwash is likely from the middle Pleistocene Lamoille glacial advance.

Cosmogenic 10Be exposure ages of boulders atop a Qgo_2 surface at the mouth of Boulder Creek adjacent to the East Humboldt Range have two groupings of ages (Zuza et al., 2021a). A grouping of three boulders with minimum ages ranging from 130–120 ka, which corresponds with previously published dates from glacial deposits of the penultimate glaciation in the Ruby Mountains–East Humboldt Range (Laabs et al., 2020). This is the preferred age for the Qgo_2 geomorphic surface at Boulder Creek and suggests that the outwash surface is correlated to the Lamoille glaciation (as termed by Sharp, 1938). Another grouping of three boulders on the Boulder Creek surface have ages ranging from 31–23 ka, which suggest that the Qgo_2 surface was not entirely abandoned during the Angel Lake glaciation. Seven additional boulders were sampled from a correlative Qgo_2 surface at the mouth of Greys Creek with a grouping of 5 boulders with ages ranging from 204–124 ka.

Qgm_2 Glacial moraine deposits, Lamoille age (middle Pleistocene) Deposits of poorly sorted sand, gravel, and boulders up to 6 m in diameter forming lateral moraines likely from the middle Pleistocene Lamoille glacial advance, moraine crests shown. Includes subangular to subrounded clasts of mylonitic quartzite, gneiss and granitic rocks. Moraine crests are rounded with fewer boulders exposed on the crest than Qgm_1.

Quaternary Tephra

Qva Vitric ash (early Pleistocene) Lenticular deposit of white to light-gray vitric ash interbedded in the lower part of an exposure of the older alluvial-fan deposits (QTa). Thickness is up to 10 m. Bedding and slump structure are present in thicker parts of the deposit and indicate fluvial reworking and redeposition. An $^{40}Ar/^{39}Ar$ analysis on sanidine from sample of the vitric ash yielded an age of 2.35±0.07 Ma (H21-SP44; Snoke et al., 2022). Chemical tephrochronology indicates correlation with the 2.1 Ma Huckleberry Ridge Tuff erupted from the Yellowstone Plateau volcanic field (Snoke et al., 2022; Christiansen, 2001; Lanphere et al., 2002).

Quaternary and Tertiary Fault Breccia

QTbx Fault breccia (Quaternary? to Miocene) Undivided fault breccia, commonly silicified. Spatially associated with mapped faults, and mapped separately from bedrocks units when the protolith unit was impossible to discern or when the unit was an exceptionally thick fault breccia.

TERTIARY VOLCANIC AND SEDIMENTARY ROCKS

Eocene through Pliocene sedimentary and volcanic deposits comprise most of the Cenozoic rocks of this compilation. The Eocene through Oligocene rocks accumulated in paleovalleys in the northern East Humboldt Range, the Wood Hills, and at Nanny Creek in the Pequop Mountains. These areas have similar stratigraphy consisting of basal conglomerate, one or two rhyolitic ash-flow tuffs, and andesite to dacite lavas. The Miocene rocks are thickest in the northern East Humboldt Range, where they were deposited in a developing half graben superposed on the paleovalley. The combined Eocene through Miocene rocks there are ~6,000 m thick, form a continuous, steeply east-dipping sequence, and are divided into 13 map units. The units in that area are, from oldest to youngest: (1) thin, unmapped basal conglomerate, (2) Eocene, 40.2 Ma tuff of Big Cottonwood Canyon (Tbcc); (3) Eocene, ca. 39.5 Ma andesite lava (Ta); (4) Eocene to Oligocene volcaniclastic sedimentary rocks (Tvs, including a 28.9 Ma marker bed, the tuff of Campbell Creek, Tcc); (5) Oligocene(?) to Miocene Paleozoic-clast conglomerate (Tso_1); (6) early(?) to middle Miocene megabreccia (Tmb) in a matrix of fine, lacustrine sediments (Tso_2); (7) middle Miocene upper conglomerate (Tso_3); (8) middle Miocene lower part of Humboldt Formation (Th_1); (9, 10) middle Miocene (15.4 Ma) Jarbidge-type rhyolite consisting of two petrographic types, finely (Tjrf) and coarsely (Tjrc) porphyritic; (11) middle Miocene (15.3 Ma) basaltic andesite lava (Tbl_2); (12) middle Miocene main part of Humboldt Formation (Th_2), and (13) upper Miocene tuffaceous sediments of the upper part of the Humboldt Formation (Th_3).

Whole-rock geochemical analyses were conducted for most of the igneous units across the map area. Complete data tables for these analyses can be found in the original references of Zuza et al. (2018, 2019, 2020, 2021a, 2022).

Tg Tertiary fanglomerate (Pliocene to Miocene?) Exposed along the western flanks of the northern Pequop Mountains and Wood Hills. In the Pequop Mountains, coarse gravel mostly expressed as a lag of boulders to pebbles of limestone, marble, and quartzite. Scattered outcrops show poorly bedded, poorly to moderately sorted, strongly to moderately calcite-cemented, fluvial gravel. Larger clasts are subangular to rounded, whereas smaller clasts are angular to subangular. Common imbrication of platy limestone and marble clasts indicates westward paleocurrents. Relative abundance of carbonate versus quartzite clasts varies north to south and probably reflects variable amount of quartzite exposure in drainages at the time, which seem to largely coincide with modern drainages. Discontinuous gravel lenses are interbedded near the top of the upper part of Humboldt Formation (Th_3), and gravel becomes predominant in the upper 10 m of the deposit. Maximum exposed unit thickness is 90 m. Younger than ca. 4.8 Ma, the weighted mean $^{40}Ar/^{39}Ar$ age of a group of the three youngest detrital sanidine grains (4.5, 5.2, and 5.7 Ma) out of 24 analyzed from an interbedded tephra (Zuza et al., 2019). Possibly younger than the ca. 4.5 Ma age of the youngest grain.

A Tg deposit exposed on the west side of the Wood Hills includes conglomerate, breccia, and sandstone with clasts derived from unmetamorphosed middle to upper Paleozoic carbonate strata that are not currently exposed in the adjacent Wood Hills. This deposit may record unroofing and erosion of unmetamorphosed Paleozoic strata in the upper plate of the REWP MCC.

Tls, Th_3, Th_2, Th_1, Th Humboldt Formation (late to middle Miocene) Heterogenous sequence of sandstone, siltstone, conglomerate, tephra (pyroclastic-fall deposits), minor diatomite, and lacustrine limestone comprise the upper (Th_3), middle (Th_2), lower (Th_1), and undivided Humboldt Formation (Th) and crops out across the map area. The individual parts are distinguished by stratigraphic position, relationship to Jarbidge-type rhyolites (Tjrc, Tjrf) where present, and $^{40}Ar/^{39}Ar$ dates (table 1). Contact between Th_3 and underlying Th_2 is poorly located in the northeastern part of the East Humboldt Range, the only area where they are exposed together. The stratigraphically middle Th_2 is separated from Th_1 by 15.4 Ma Jarbidge-type rhyolite lavas in the Welcome and Humboldt Peak quadrangles (McGrew and Snoke, 2015; McGrew, 2018). Throughout Th, sandstone and siltstone commonly are tuffaceous and planar-bedded to thinly laminated.

Unit Th_3 is exposed in the Welcome quadrangle in the northern East Humboldt Range and in the Independence Valley NE quadrangle along the western edge of the Pequop Mountains; it is distinguished by late Miocene, ≤12 Ma, dates on primary and reworked tephra. New $^{40}Ar/^{39}Ar$ dates bracket the age of Th_3 between approximately 6 Ma and 11.7 Ma (table 1).

In the Welcome quadrangle, where it is at least 1,300 m thick, unit Th_3 consists of predominantly soft, poorly exposed tuffaceous sediments and primary to variably reworked pyroclastic-fall deposits (tephra). The base is taken to be slightly below a tephra deposit with a sanidine $^{40}Ar/^{39}Ar$ date of 11.67±0.02 Ma (H23-W377; table 1). Deposits are generally thinly to thickly bedded and locally calcite-cemented or altered to clay. Glass shards and sanidine and quartz phenocrysts are easily observable with a hand lens in coarser deposits. Minor soft-sediment deformation. In addition to the above date, tephra sample H23-W373 yielded a sanidine date of 10.89±0.03 Ma from a stratigraphically higher bed. These dates and sanidine K/Ca ratios indicate the two beds are distal fall deposits of the Cougar Point Tuffs III and XIII (Bonnichsen et al., 2008). Zircon fission-track dates from vitric ash are 8.3±0.9 Ma (WE-1, same location as H23-W377, Mueller, 1992) and 11.9±0.9, 8.9±0.7, 11.9±1.0, and 11.1±0.9 Ma) in the Oxley Peak quadrangle immediately north of this map area (R.A. Zimmermann, in Thorman et al., 2003).

In the western Pequop Mountains, unit Th_3 is approximately 350 m thick in the footwall of the Independence Valley fault zone. The lower part is light-colored, variably calcite-cemented, shard-rich sandstone, siltstone, pebble conglomerate, and minor tuff. Sandstone is thick- to thin-bedded, and siltstone is platy bedded. Sandstone locally contains pumice up to 1 cm diameter. The upper part is light brown, massive to rarely thick- to medium-bedded, weakly calcite-cemented sandstone that contains sparse, matrix-supported clasts of quartzite, limestone, and marble to 15 cm. Irregularly bedded, white to cream-colored lacustrine limestone is locally exposed in both parts. The upper part of the brown sandstone is ca. 6.04±0.09 Ma, the weighted mean $^{40}Ar/^{39}Ar$ age of a homogeneous population of 20 of 23 analyzed sanidine grains from a tuff-rich bed (sample H17-66; table 1). $^{40}Ar/^{39}Ar$ dates on three samples of the lower part range from ca. 10.8 to 9.9 Ma. Outcrop sample H17-53 yielded a weighted mean age of 10.31±0.03 Ma from a coherent group of 6 sanidine grains out of a total of 24 analyzed grains; older grains range from 10.36 to 38.88 Ma (table 1). Two samples from drillhole WNC119 yielded ages of 9.90±0.13 Ma (WNC119-34 foot depth; 5 sanidine grains out of 24, the rest of which are plagioclase) and 10.74±0.03 Ma (n = 3 of 24) and 10.78±0.03 Ma (n = 3 of 16) (WNC119-425 foot depth, separately prepared aliquots analyzed in 2018 and 2016; table 1).

A megabreccia-containing landslide deposit (Tls) underlies and is partly interbedded with Th_3 in the scarp and uplifted footwall of the Independence Valley fault zone. Individual large blocks, a minimum of about 8 m in diameter, commonly several tens of meters in diameter, and reaching 230 m long are mapped separately and identified by their primary rock type. Individual blocks are identified by continuity of bedding orientation over the entire block but are commonly brecciated at their margins. Rock types comprising individual blocks are Eureka Quartzite (Oe), undivided Pogonip Group (Op), Notch Peak Formation (O€np, distinguished by common dolomite and abundant, thin chert layers), and jasperoid (probably silicified Pogonip Group limestone) and undivided limestone, commonly showing small-scale internal folds. The individual blocks are the same units and have textural characteristics similar to rocks exposed along the western edge of the present Pequop Mountains, which allows them to be derived from there. Exposed thickness ranges from 20 m to 90 m. Age ca. 11–10 Ma based on age of surrounding tephra, which distinguishes Tls from the lithologically similar but older, ~17–16 Ma Tmb in the East Humboldt Range.

Unit Th_2 is exposed in all three ranges and is lithologically similar to unit Th_3. In the Welcome quadrangle, where it is about 1,500 m thick, and we examined most extensively, it has more sandstone and numerous conglomerate lenses and, in the lower part, basaltic andesite lavas (unit Tbl_2). Sandstones vary from consisting mostly of unmetamorphosed Upper Paleozoic grains to predominantly tuffaceous with few, if any, bedrock grains. Lenticular conglomerate beds are 30 to 80 m long and 2–5 m thick, which suggests channels in finer deposits. Clasts are well-rounded, up to 20 cm in diameter, and consist of unmetamorphosed Paleozoic rocks, including Diamond Peak Formation and Eureka Quartzite, and Jarbidge-type rhyolite. A coarse conglomerate, the boulder conglomerate map unit of McGrew and Snoke (2015), in the lower part of Th_2 contains boulders up to 1.2 m of Jarbidge-type rhyolite and coarsely plagioclase-phyric basaltic andesite that is petrographically, chemically, and age indistinguishable from rock that makes up the in situ lavas (unit Tbl). Boulders reside in white, calcareous soil, presumably weathered from conglomerate matrix. Plagioclase from a basaltic andesite clast yielded a $^{40}Ar/^{39}Ar$ date of 15.46±0.06 Ma (H14-107; table 1).

Unit Th_2 deposits are similar in the Wood Hills and northern Pequop Mountains, which also have minor lacustrine limestone. A zircon fission-track date of 11.6±1.2 Ma at the top of exposed Th_2 in the Wood Hills (Camilleri, 2010) could put a small part of that map polygon in unit Th_3, which we have not done. Camilleri (2010) noted that clasts are entirely unmetamorphosed Upper Paleozoic rocks except at the level of the fission-track dated tephra, where metamorphic clasts similar to metamorphic rocks in the Wood Hills are present.

Unit Th_1 consists of fine conglomerate, sandstone, and tuffaceous sediments and is distinguished by its stratigraphic position below Jarbidge-type rhyolite, which is only present in the East Humboldt Range. The base of Th_1 is marked by an increase in the tuffaceous component of deposits compared to the underlying upper conglomerate (Tso_3). Anorthoclase from a minimally reworked tephra in the lower part in the northeastern East Humboldt Range yielded a $^{40}Ar/^{39}Ar$ date of 15.62±0.12 Ma (H5EH-118, table 1). This is probably a depositional age because the age and K/Ca closely match those of the Cold Springs tuff in the Santa Rosa Range (Brueseke et al., 2008) 200 km to the west, which would have been upwind. Four of 89 analyzed sanidines from a highly reworked tephra in the Humboldt Peak quadrangle yielded a maximum depositional age of 15.71±0.11 Ma (040731-1A).

Undivided Th in the Heelfly Creek quadrangle in the western East Humboldt Range both under- and overlies rhyolite lava (Tjrc), and $^{40}Ar/^{39}Ar$ dates on tephra range from 15.77±0.02 to 8.30±0.20 Ma, with a reworked deposit no older than ~5.15±1.80 Ma. This range indicates all parts of the Humboldt Formation are present, but poor exposure and implied repetition by major but unmapped faults preclude distinguishing them.

The Humboldt Formation is also interpreted to fill the late-Cenozoic depocenters in Independence and Clover valleys, where it may exceed 2 km thick based on regional gravity modeling.

Tbl_2 Basalt lava, Unit 2 (middle Miocene) Dark, coarsely plagioclase-phyric to aphyric basaltic andesite lavas overlie Jarbidge-type rhyolite in the northeastern East Humboldt Range. Flows are commonly scoriaceous and amygdaloidal. The coarsely porphyritic type has 5–15% glassy plagioclase up to 2.3 cm long and clinopyroxene. The lavas are tholeiitic with 55–56% SiO_2 and 12% FeO. Plagioclase $^{40}Ar/^{39}Ar$ date of 15.33±0.05 Ma (H14-92, Welcome quadrangle). $^{40}Ar/^{39}Ar$ dating of basaltic lavas and dikes in the East Humboldt Range area reveal two age clusters, ca. 16.9 and 15.4 Ma. Unit Tbl_2 lavas and possibly some dikes outside the map area near Harrison Pass that yielded whole rock $^{40}Ar/^{39}Ar$ dates of 15.50±0.10 and 15.54±0.10 Ma on a single dike (RM643 A,B, Hudec, 1990) constitute the younger episode.

Tmb_2 Megabreccia, Unit 2 (middle Miocene) Light gray to cream-colored fractured and silicified megabreccia that consists of upper Paleozoic carbonates, sandstone, and lesser conglomerate. Found in the western Wood Hills. Despite pervasive fracturing and veining, primary bedforms such as cross-bedding are still observed. Silicified megabreccia defines ridgetops with large (>10 m) outcrops.

Tjrf, Tjrc Jarbidge-type rhyolite (middle Miocene) Finely (Tjrf) and coarsely (Tjrc) porphyritic Jarbidge-type rhyolite lavas that are orange- to pinkish-gray crop out in the western and eastern sides of the East Humboldt Range as far south as Secret Pass. Where both units are exposed together, the finely porphyritic rhyolite overlies the coarsely porphyritic rhyolite. Both units contain 25–30% phenocrysts of distinctive smoky quartz, potassium feldspar (definite anorthoclase and possible sanidine), plagioclase, clinopyroxene, and generally altered mafic minerals that could be orthopyroxene or fayalite (Fe-rich olivine). Phenocrysts are generally less than 2 mm in diameter in finely porphyritic rhyolite and commonly 6 mm and up to 12 mm in diameter in coarsely porphyritic rhyolite. Thickest deposits are in the northeastern East Humboldt Range, where the two units aggregate ~1,300 m. Several lavas of Tjrc in the western East Humboldt Range are up to ~30–50 m thick and are interbedded with undivided Humboldt Formation (Th). Tjrf is discontinuously and commonly poorly exposed in the southwestern East Humboldt Range. It is up to 10 m thick and has a thin, poorly exposed basal vitrophyre overlain by massive, devitrified rock. Lavas commonly have a black basal vitrophyre up to 4 m thick that is overlain by massive to strongly flow-banded and locally columnar-jointed, devitrified rock.

Phenocryst phases in both rhyolite types are rounded and embayed, with pockets of matrix in the phenocrysts. Plagioclase is faintly albite-twinned, whereas anorthoclase is more strongly grid-twinned. K/Ca of grains analyzed for $^{40}Ar/^{39}Ar$ dating is ~10, confirming anorthoclase. Glomerocrysts of anorthoclase, clinopyroxene, and opaque minerals (Fe-Ti oxides) occur in both rock types. Clinopyroxene has reaction rims with matrix. Microlites of feldspar laths are common in the glassy matrix of vitrophyres. Chemical analyses show the rocks are Fe-rich rhyolites with ~75–76% SiO_2 (Dee et al., 2015).

The rhyolites are the southwesternmost known occurrences of Jarbidge-type rhyolites, which have the same distinctive phenocrysts and chemical characteristics (Coats, 1987; Brueseke et al., 2014). Jarbidge Rhyolite is most extensive near Jarbidge, NV, near the Idaho border, where individual flows are more than 200 m thick, cumulative sections are at least 480 m thick, and total volume is estimated to be 500 km^3 (Brueseke et al., 2014). Anorthoclase $^{40}Ar/^{39}Ar$ dates are 15.35±0.01 Ma and 15.37±0.04 Ma for Tjrc (H14-52, western Tent Mountain quadrangle) and Tjrf (H14-54, northwestern Secret Valley quadrangle), respectively (Zuza et al., 2021a), and 15.35±0.04 Ma (Tjrc, Welcome quadrangle; M. Brueseke, personal communication. in McGrew and Snoke, 2015). These dates overlap other $^{40}Ar/^{39}Ar$ (Brueseke et al., 2014) and K-Ar (Coats, 1987) dates from Jarbidge-type rhyolites in the Jarbidge area.

Tbl_1 Basalt lava, Unit 1 (middle Miocene) Massive to moderately vesicular basalt forms The Mound, a ~300 m wide, 20 m high remnant of a probable lava surrounded by Quaternary deposits in Clover Valley. Phenocrysts consist of sparse, commonly large (to 2.5 cm) plagioclase, clinopyroxene, olivine, and magnetite. The Mound is tholeiitic with 53% SiO_2 and 9.5% FeO. Matrix and plagioclase $^{40}Ar/^{39}Ar$ dates of 16.92±0.04 and 16.68±0.08 Ma (H14-66, table 1) place it in the older group of basaltic rocks emplaced during initial extension.

Clover Creek sequence, northern East Humboldt Range

Tso_3 Older sedimentary deposits, Unit 3 (middle Miocene) Heterogeneous sequence of interbedded conglomerate, sandstone, siltstone, and lacustrine limestone. Conglomerates make dark stripes within light-colored, finer deposits and decrease in abundance and thickness upward. Conglomerates near the base are indurated (silica- or ferruginous-cemented), massive to thick-bedded, as much as 5 m thick, and contain poorly sorted, moderately rounded clasts of unmetamorphosed Paleozoic rocks (e.g., chert-pebble conglomerate from the Diamond Peak Formation, limestone, and quartzite) and minor andesite and white, porphyritic tuff from 1 cm up to 25 cm in diameter. Maximum clast size decreases to about 5 cm in the middle part of the unit, where conglomerates are calcite-cemented. Calcite-cemented sandstones and siltstones and thin-bedded to laminated limestones occur throughout the sequence. Sandstone grains are mostly well-rounded quartz and dark chert, with some sanidine. Conglomerate, sandstone, siltstone, and limestone appear to form fining upward sequences at several stratigraphic levels. Thickness ~700 m along section A. Age: Detrital sanidine grains from a calcareous sandstone about 20 m above the base (H21-W206A) yielded a maximum depositional age of 21.2±0.1 Ma (2 of 119 grains). Detrital sanidine and zircon grains from a calcite-cemented, pebble conglomerate to sandstone lens in the upper part (H21-W219) yielded a maximum depositional age of 16.36±0.03 Ma (sanidine, 1 of 375 grains) and 16.6±0.2 Ma (zircon, 8 of 107 grains).

Tso_2, Tmb_1 Older sedimentary deposits, Unit 2, and Megabreccia, Unit 2 (middle Miocene) Unit Tso_2 is the “matrix” of sandstone, siltstone, lacustrine limestone, and minor conglomerate that overlies the Paleozoic-clast conglomerate (Tso_1) along a sharp, planar contact and contains abundant, individually mapped megabreccia (Tmb_1)–large blocks, up to 200 m long and forming resistant knobs. Breccia blocks are unmetamorphosed Upper Devonian Guilmette Formation with lesser sandstone and dolomite bodies interpreted as Middle Devonian Simonson Dolomite. The largest individual blocks have shattered–brecciated rims up to several meters thick surrounding more coherent cores; some smaller blocks, up to ~5 m in diameter, are entirely brecciated.

Interbedded, mostly poorly exposed fine deposits consist of thick- to thin-bedded to platy, calcite-cemented, coarse to medium sandstone, siltstone, and limestone. Grains are variable proportions of quartz, sanidine, and dark chert. Pebble to cobble conglomerate beds are scattered through the lower and middle part of the unit. Clasts in stratigraphically lower conglomerates are well rounded, dark chert and probably are continuations of Tso_1 deposition. Clasts in stratigraphically higher conglomerates are mostly limestone (Guilmette?). Limestone layers contain gastropods and ostracods as well as unidentified dark rods.

Unit Tso_2 is as much as 1,300 m thick in the central part of its distribution west of Clover Hill, where evidence for repetition by faulting is absent. The unit thins and wedges out 3.3 km to the north in Clover Creek.

Unmetamorphosed carbonates that could be sources for the megablocks are exposed in the northwestern Wood Hills (Thorman, 1970; Camilleri, 2010) and southern end of Clover Hill (McGrew, 2018). The megabreccia blocks are interpreted as rock-avalanche deposits derived from substantial relief generated during active normal faulting (e.g., McGrew and Snoke, 2015) and shed into a normal fault-bounded, lacustrine basin in which the finer deposits were accumulating. Based on their stratigraphic position toward the bottom of the Miocene section, these megabreccia deposits may record initial or early extension, normal faulting, and relief generation.

The age of this unit is only loosely constrained to early to middle Miocene based on detrital sanidine $^{40}Ar/^{39}Ar$ and zircon U-Pb dating of sandstones. Specifically, this deposit is younger than the youngest ca. 21 Ma dated grains from samples in the unit but older than the ~16.4 maximum depositional age of unit Tso_3. In ascending stratigraphic order: H21-W178 (youngest sanidine 21.84±0.03 Ma; youngest zircon 21.4±1.0 Ma); H21-W162 (youngest sanidine 23.90±0.01 Ma; youngest zircon 21.0±1.4 Ma); H21-W165 (youngest sanidine 23.89±0.07 Ma); H21-W174 (youngest sanidine 23.02±0.04 Ma; youngest zircon 21.1±1.2 Ma). These ages probably reflect what was available to be reworked into the sandstones rather than their depositional age. We suggest the depositional age is closer to ca. 17 Ma, which would support a more continuous stratigraphy as part of the middle Miocene Humboldt Formation and coincident with the beginning of major extension in the region (Colgan and Henry, 2009; Colgan et al., 2010; Henry et al., 2011). Conversely, an interpretation of an early Miocene age for this deposit implies a hiatus between megabreccia generation and subsequent deposition of the overlying, thicker middle Miocene Humboldt Formation.

Tso_1 Older sedimentary deposits, Unit 1 (late Oligocene? to middle Miocene) Massive to thick-bedded, pebble conglomerate composed primarily of Paleozoic clasts up to 5 cm in diameter overlies the volcaniclastic sedimentary rocks along a gradational, irregular contact. Clasts are unmetamorphosed, mostly dark chert and dark siliceous argillite (probably from Chainman Formation), lesser quartzose sandstone and quartz-chert pebble conglomerate (probably from Diamond Peak Formation), minor limestone, and minor to absent volcanic rocks. Clasts are mostly moderately rounded but vary from angular to well-rounded in individual beds and clast-supported. Matrix-supported pebbly mudstone is minor. Age limited to between 28.9 Ma, the marker bed in the underlying volcaniclastic sedimentary rocks (Tvs) and 16.4 Ma, the maximum age of unit Tso_3.

Tso Older sedimentary sequence, undivided (to middle to early? Miocene) Heterogeneous sequence of interbedded conglomerate, sandstone, siltstone, and lacustrine limestone. Mapped only in two areas in the northeastern and southwestern East Humboldt Range, where age relations are unknown.

Tvs Volcaniclastic sedimentary rocks (late Oligocene to late Eocene) Conglomerate and sandstone mostly composed of andesite and rhyolite ash-flow tuff clasts with minor unmetamorphosed Paleozoic rocks. Scattered layers are predominantly Paleozoic clasts. Generally, poorly exposed as a lag of clasts. Sparse outcrops are massive to thick, planar bedded. Clasts are angular to moderately rounded and mostly ≤50 cm in diameter but rarely as large as 1.4 m. Probably accumulated in a paleovalley in the Clover Creek area of the Welcome quadrangle. Overlies tuff of Big Cottonwood Canyon (Tbcc) or andesite lava (Ta) in the Welcome quadrangle, so younger than ca. 39.5 Ma. The 28.93±0.07 Ma tuff of Campbell Creek (H10-79; table 1) forms a ~50-cm-thick marker bed in the upper part of Tvs. Sparsely porphyritic with 10% phenocrysts of quartz (3%, 2 mm, distinctly vermicular “wormy”), sanidine (3%, 2 mm), plagioclase (3%, 2 mm, altered to clay), and biotite (1%, 1 mm). Erupted from a caldera in the Desatoya Mountains, ~300 km to the southwest (Henry et al., 2012). Unit Tvs is overlain by the undated Paleozoic-clast conglomerate (Tso_1), and older than megabreccia-bearing unit (Tmb), which has a maximum age of ~20 Ma.

Tx Sedimentary breccia (middle Eocene) Thick sequence at Nanny Creek consisting of coarse breccia of blocks of tuff of Big Cottonwood Canyon (Tbcc), lesser plagioclase-biotite tuff (Tpb), and minor andesite or dacite (Ta) in a mostly nonexposed clastic to tuffaceous matrix. The blocks are as much as 10 m in diameter and much more resistant than matrix, so stand up as “haystacks”. Approximately 750 m thick. This coarse breccia results from intense erosion and reworking of the underlying rocks by “dam-burst floods”, where blockage of the paleovalley created temporary lakes that overtopped the blockage and released much larger amounts of water than in normal floods (Henry, 2008).

Txs Tuff and tuffaceous sedimentary rock (middle Eocene) A few layers of massive, to well-bedded, to platy, tuffaceous sandstone and siltstone are interbedded with sedimentary breccia (Tx) and with the andesite-dacite lava and breccia (Ta) at Nanny Creek. The deposits contain porphyritic pumice, abundant quartz and feldspar mineral fragments, and sparse ash-flow tuff clasts that indicate they are reworked from poorly welded upper parts of the underlying ash-flow tuffs. Mapped layers are 10 to 20 m thick.

Ta Andesite-dacite lava and breccia (middle Eocene) Flows and breccias of andesite to dacite lavas form a thick, as much as 1,200 m, sequence at Nanny Creek in the northern Pequop Mountains and thin sequences in the northern East Humboldt Range, Secret Valley, and Wood Hills. In all areas except Secret Valley, the lavas overlie the tuff of Big Cottonwood Canyon, fill paleovalleys, and vary in thickness along strike because of irregular deposition and erosion. At Nanny Creek, lavas underlie and are partly interbedded with sedimentary breccia (Tx). In the northern East Humboldt Range, lavas underlie volcaniclastic sedimentary rocks (Tvs).

At Nanny Creek, flows and flow breccias make relatively resistant outcrops in the lower part of the sequence in the middle of the paleovalley, whereas pyroclastic breccia is nonresistant and poorly exposed in the upper two thirds of the sequence. Pyroclastic breccias have blocks of massive, commonly glassy dacite or andesite in a fine, variably pumiceous matrix. Andesitic rocks contain plagioclase, clino- and orthopyroxene, and minor to no hornblende. Dacitic rocks contain plagioclase, common biotite and hornblende, and minor to no clinopyroxene. Sources of these rocks must be nearby, but no dikes or other possible sources have been found. Age: 39.54±0.03 Ma, biotite, H14-70 (Henry and Thorman, 2015); 39.7±0.5 Ma, hornblende, 91T10 (Brooks et al., 1995a, b).

Minor andesite lava flows, flow breccias, and volcaniclastic rocks in the Welcome and Secret Valley quadrangles of the East Humboldt Range are mostly finely porphyritic with phenocrysts of plagioclase (10–15%, 1–2mm), pyroxene (3–5%, 1mm), and, in a few flows, hornblende (0–2%, 1–3 mm). As much as 50 m thick in the paleovalley in the Welcome quadrangle.

Tbcc Tuff of Big Cottonwood Canyon (middle Eocene) Brown-weathering, light gray, densely to poorly welded, devitrified, rhyolitic ash-flow tuff that crops out near the bottom of paleovalleys in all three ranges. Phenocrysts (20–25%): quartz (6%, ~3 mm), sanidine (6–7%, ~2.5 mm), plagioclase (7–10%, ~3 mm), biotite (1%, ~2 mm), and hornblende (<1%, <1 mm), 3% pumice to 2 cm long. As much as ~100 m thick in the paleovalley in the Welcome quadrangle, where it is discontinuous along strike because of irregular deposition and erosion. Here, it locally includes a thin, unmapped, underlying conglomerate marked mostly by a lag of rounded pebbles to boulders of unmetamorphosed Paleozoic limestone, chert, and chert-pebble conglomerate along the unconformity with Permian rocks. In the Pequop Summit quadrangle, Tbcc is approximately 120 m thick and was deposited on mappable tuff (Tpb) and conglomerate (Tc). Erupted from the Big Cottonwood Canyon caldera near Tuscarora, ~100 km to the west-northwest (Henry and Boden, 1998; Castor et al., 2003; Henry, 2008). Sanidine $^{40}Ar/^{39}Ar$ dates include 40.21±0.02 Ma (H13-47, Welcome quadrangle) and 40.26±0.07 Ma in the Pequop Summit quadrangle (Henry, 2008). Brooks et al. (1995a, b) report a biotite $^{40}Ar/^{39}Ar$ date of 40.2±0.2 Ma from the outcrop in the Wood Hills. Reverse polarity (Palmer and MacDonald, 2002).

Tpb Plagioclase-biotite tuff (middle Eocene) Dark brown weathering, devitrified, densely to poorly welded rhyolitic ash-flow tuff forms a resistant ledge in the middle of the Nanny Creek paleovalley in the northern Pequop Mountains, where it overlies conglomerate (Tc). Phenocrysts (30−35%): plagioclase (25−30%, <1−3 mm), biotite (3–4%, <1–2 mm), probable clinopyroxene (altered, 2%, 1 mm), hornblende (1%, ≤1.5 mm), sanidine (0–<<1%, ≤ 0.5 mm), and quartz (0 − <<1%, 0.1 − 0.3 mm). Approximately 90 m thick. Source unknown but probably near Tuscarora based on distribution (Henry, 2008). Plagioclase $^{40}Ar/^{39}Ar$ dates include 40.95±0.13 Ma and 41.61±0.22 Ma (Henry and Thorman, 2015).

Tc Conglomerate (Eocene or older) Conglomerate mapped only within the Nanny Creek paleovalley in the Pequop Summit quadrangle but also present as thin, unmapped lenses underlying tuff of Big Cottonwood Canyon in the northern East Humboldt Range and in the Wood Hills. Consists of coarse to extremely coarse gravel and conglomerate that is probably predominately Eocene, but some gravels could be as old as Late Cretaceous. The unit consists of residual boulders with no exposed matrix that occupies the center of the paleovalley, where it underlies the plagioclase-biotite tuff. Boulders are rounded, commonly to

1.7 m in diameter, and consist mostly of chert-pebble conglomerate derived from the Diamond Peak Formation. Other clasts are quartzite, Jurassic granodiorite, chert, minor crinoidal limestone, and very sparse ostracod-bearing limestone that is characteristic of Eocene deposits in northeastern Nevada (Brooks et al., 1995b). Approximately 40 m thick.

CENOZOIC AND MESOZOIC INTRUSIVE ROCKS

Tjrd Jarbidge-type rhyolite dikes (middle Miocene) Two finely porphyritic rhyolite dikes with phenocrysts of quartz (1–2 mm) and altered sanidine intruded lower plate mylonitic rocks around Clover Hill. The phenocrysts and a chemical analysis indicate the dikes are part of the finely porphyritic Jarbidge-type rhyolite (Tjrf) and are likely the same age, ca. 15.4 Ma. The dikes are undeformed, which implies that shearing had ceased by the time of dike intrusion. The dikes could be local feeders to exposed finely porphyritic Jarbidge rhyolite lava (Tjrf), whose source is otherwise unknown. Furthermore, although the source for much of the thick rhyolite lava flows (Tjrf and Tjrc) remains unknown, the observation of intrusive rhyolite dikes implies that the lavas could have erupted from a local source.

Tbd Basalt dikes (middle Miocene) Dark gray-black, generally undeformed, nonfoliated, microcrystalline tholeiitic basalt to basaltic andesite. Mostly observed as north-northwest striking dikes, ≤ 1 to 5 m wide, discordantly crosscutting adjacent units including mylonitic foliations. Local chilled margins and commonly poorly exposed. In the southwestern part of the East Humboldt Range, basalt dikes intrude parallel north-northwest striking fault zones, indicating that the faults are older or likely synchronous with the basalt dikes. SiO_2 contents of analyzed rocks including contemporaneous lava form three clusters, 48% (Angel Lake dikes), 52.5% (The Mound; unit Tbl_1), and 57% (Tent Mountain dike), which may reflect variable differentiation. The basalt dikes cut across metamorphic and mylonitic foliations but are truncated by the Ruby Mountains–East Humboldt Range detachment fault, thus constraining mylonitic shearing to pre-17 Ma and detachment faulting to post-17 Ma. A matrix $^{40}Ar/^{39}Ar$ date of 16.85±0.10 Ma (H14-55, Tent Mountain dike; table 1) and a plagioclase $^{40}Ar/^{39}Ar$ date of 17.3±0.3 Ma (H15-34, Angel Lake dike) indicate they are part of the older episode of basaltic magmatism related to initial extension.

Tmg Biotite monzogranite orthogneiss (early Oligocene to middle Eocene) Moderately to strongly foliated, moderately to strongly lineated, medium-grained, equigranular biotite monzogranite and lesser tonalite and granodiorite (Batum, 1999). Found in the Ruby Mountains and East Humboldt Range. Contains approximately 10% biotite and subequal proportions of oligoclase, alkali feldspar, and quartz. Commonly forms tabular sheets that are concordant to slightly discordant, up to 70 m thick but typically 1–10 m. Forms prominent blocky dark gray to dark brown cliffs. Less deformed at deeper structural levels, where Tmg crosscuts preexisting fabrics as dikes. U-Pb zircon dates are ca. 31–29 Ma (Wright and Snoke, 1993; Zuza et al., 2022).

Trd Rhyolite dikes (Eocene) Tan-weathering, sparsely porphyritic, and mostly non-resistant rhyolite sills and dikes intrude rocks of the Killian Springs Formation (Ꞓks) and Toano Limestone (Ꞓt) in the Pequop Mountains. Contacts and igneous foliations partly parallel host-rock foliations and partly crosscut them. Fewer than 1% phenocrysts of quartz and altered feldspar up to about 1 mm in diameter occur in a fine-grained matrix of quartz and feldspar with alteration products of sericite (muscovite?) or clay. Bedell et al. (2010) reported U-Pb zircon dates of 39.1±0.7 Ma and 41.0±0.8 Ma.

Tlg Leucogranite (Eocene) Equigranular medium-fine grained muscovite leucogranite. Contains plagioclase feldspar, K-feldspar, quartz, and muscovite, with lesser garnet and biotite. Exhibits strong foliation and lineations. Exposed as foliation-parallel lenticular sheets 5–10 m thick. This unit includes the muscovite leucogranite orthogneiss of Woods Creek of Sicard and Snoke (2020). U-Pb zircon dating suggests an age of 39.8 +/- 1.0 Ma (Zuza et al., 2021a).

Tgd Granodiorite (Eocene) Sill of equigranular granodiorite with no evidence for crystal-plastic deformation that intruded strongly mylonitic Paleozoic marbles and siliciclastic rocks in the southwest corner of the map area. Unit is fractured, brecciated, and chlorite-altered, probably due to nearby structurally higher detachment fault. Rock is similar to granodiorite rocks that are associated with the Eocene (ca. 36 Ma) Harrison Pass pluton (Barnes et al., 2001) to the south in the Ruby Mountains. Tgd is less felsic than the other Tgo and Tmg phases with ~68% SiO_2 (Zuza et al., 2021a). U-Pb zircon dating yielded an Eocene age of 39.1±1.2 Ma (Zuza et al., 2021a, 2022).

The Eocene age and field relationships for this unit imply that some mylonitic shearing occurred prior to the middle Eocene, which could be related to an early Cenozoic phase of extensional shearing or an older Mesozoic deformational event. We interpret that this unit and the rocks it intruded came from a higher structural position that was not impacted by Oligocene mylonitic shearing, and was subsequently detachment-faulted down to its current structural position in the middle Miocene.

Tgo Granitic orthogneiss (Eocene) Moderately foliated, usually weakly lineated coarse-to-medium grained monzogranitic orthogneiss composed of plagioclase, K-feldspar, quartz, biotite, and muscovite. The unit is distinctive with relatively large (~1–2 cm) plagioclase porphyroclasts. Commonly, chlorite-altered and exposures may have a green hue. The unit intrudes relatively structurally higher levels of the lower plate, including the Paleozoic marbles, and is rarely found within the ЄZpm or structurally deeper rocks. This unit includes biotite granodiorite–monzogranite orthogneiss of Horse Creek of Sicard and Snoke (2020). U-Pb dating yielded an Eocene 38.9±1.2 Ma age for this unit (Zuza et al., 2021a), overlapping ages of Tqd and Tgd.

Tqd Hornblende-biotite quartz diorite (middle Eocene) Weakly to strongly foliated, weakly to strongly lineated, porphyritic appearance with 1–2 mm plagioclase, with lesser hornblende, biotite, and quartz. Conspicuously less foliated, lineated, and sheared than adjacent metamorphosed rocks, possibly due to its greater strength than the other units. Geochemical analyses show ~60–65% SiO_2 (Zuza et al., 2021a). Forms dark gray-black, jagged, high-relief cliffs that commonly define ridges. Mostly subparallel to dominant foliation, but also discordant to oblique to primary foliation. Intermingled with TKlg, and crosscut by Tmg and a late undeformed TKlg. Ridges and dip slopes commonly consist of intermingled Tqd and lesser TKlg. The intrusions tend to concentrate in OЄmi, close to the contact with the underlying ЄZpmi paragneiss. Defines the major north-trending ridgeline of Hole in the Mountain Peak, separating Lizzies Basin on the east from the Boulder Creek drainages on the west. U-Pb zircon dating suggests an age of ca. 40 Ma (Wright and Snoke, 1993; Zuza et al., 2021a, 2022).

TKlg Leucogranite and leucogranitic orthogneiss (Oligocene to Cretaceous) Weakly to strongly foliated, coarse to medium-grained, commonly pegmatitic, leucogranite. Includes lesser trondhjemitic pegmatite, muscovite-rich two-mica leucogranite, and weakly foliated, fine- to medium-grained late-stage garnet aplite dikes (Batum, 1999). Mylonitic fabrics indicate west- to northwest-directed shear. Foliated leucogranite commonly forms discontinuous meter to sub-meter scale concordant sheets, pods, or lenses throughout the rocks in the metamorphic core complex. Mappable lenses of TKlg are up to 50 m thick. Weakly foliated aplite dikes obliquely cut foliation. A leucogranite in the Welcome quadrangle to the northeast yielded a $^{207}Pb/^{206}Pb$ zircon date of 85 ± 3 Ma (Snoke et al., 1990, and McGrew and Snoke, 2015), similar to leucogranite ages from the southern East Humboldt Range and Ruby Mountains (e.g. Snoke et al., 1990). Hallett and Spear (2015) presented ca. 80 Ma U-Pb monazite ages from leucosome sampled from the Winchell Lake nappe in the Humboldt Peak quadrangle.

Most leucogranite is interpreted to be Late Cretaceous (Wright and Snoke, 1993; McGrew et al., 2000), but observations of TKlg intermingled with, or directly crosscutting, the Cenozoic Tqd and Tmg intrusions require that the TKlg age range extends to as young as Oligocene (e.g., McGrew, 2018). One medium grained muscovite-garnet leucogranite in the southwestern East Humboldt Range yielded a U-Pb zircon 36.8±1.0 Ma (Zuza et al., 2021a). This age is slightly younger than most of the other middle Eocene igneous rocks in the map area, and thus may represent protracted heating and partial melting.

Kg Leucogranite, undeformed (Late Cretaceous) Relatively undeformed white leucogranite pods and sills in the Wood Hills and northern Pequop Mountains. Fine- to coarse-grained leucogranite with quartz, microcline, plagioclase, muscovite, and minor garnet. Kg intruded Ordovician–Devonian strata in the Wood Hills and Cambrian strata in the Pequop Mountains. Based on a discordant age population of zircons from a sample in the Pequop Mountains, Bedell et al. (2010) concluded that the leucogranite is no older than Late Cretaceous. $^{40}Ar/^{39}Ar$ step-heating of muscovite from several samples suggest that they are Late Cretaceous, cooling through muscovite closure temperatures at 70–85 Ma (Henry and Thorman, 2015; Zuza et al., 2019).

Jl Mafic dikes and sills (Jurassic) Lamprophyre and monzodiorite to gabbro dikes and sills are distributed across the Pequop Mountains. Lamprophyres make thin (0.2- to 3-m-thick to >100-m-long) sills generally parallel to metamorphic foliation but locally form similarly thin dikes that cut the foliation. A lamprophyre intruded along the Independence thrust fault in the west-central part of the quadrangle indicates the thrust is older. Most lamprophyres are strongly altered to light to dark brown with all primary minerals destroyed. Where less altered, abundant hornblende or clinopyroxene phenocrysts reside in a groundmass of feldspar and quartz. Monzodiorite and one gabbro make thicker, more irregular intrusions up to ~100 m long comprised of equigranular medium-grained hornblende, biotite, plagioclase, and clinopyroxene, which suggest they are coarser, more slowly cooled versions of lamprophyre. Age constraints on these intrusions include a U-Pb zircon age from the gabbro of 159±6 Ma (sample PQSG) (Bedell et al., 2010), hornblende $^{40}Ar/^{39}Ar$ ages of 160.9±0.5 Ma (isochron) on a sample from the Long Canyon Mine (sample H14-64), and hornblende 40Ar/39Ar ages of 161.5±0.2 Ma and 159.6±0.2 Ma (plateaus) from a relatively unaltered lamprophyre dike in the Independence Valley SE quadrangle (Zuza et al., 2020).

Jg Granitic (or rhyolitic) sills (Jurassic) In the Pequop Mountains, Jg consists of fine-grained, tan-weathering sills that form a mostly north-northeast-striking belt across the northern half of the Independence NE quadrangle. Variably sericitized plagioclase grains up to 2 mm long and completely altered biotite(?) up to 1 mm long are the only phenocrysts in a fine-grained matrix of quartz, plagioclase, orthoclase, sericite, and opaque minerals including former pyrite. A sill in Meyers Canyon forms a series of boudins as much as 3 m thick and 12 m long surrounded by marble (Clifside Limestone) whose foliation wraps around the boudins. Zuza et al. (2021b) dated this sill and reported a U-Pb zircon age of 155.6±0.8 Ma from 13 concordant zircon analyses.

In Secret Valley, the Jg is granite consisting of fine-grained feldspar and quartz matrix with muscovite phenocrysts (~3 mm in diameter) and smaller feldspar microphenocrysts. This unit intruded unmetamorphosed Ely Limestone. The granite is approximately 161 to 154 Ma as determined via Rb-Sr muscovite whole-rock isochron age and K-Ar muscovite dating (dates reported in Dallmeyer et al., 1986).

UNMETAMORPHOSED PALEOZOIC SEDIMENTARY ROCKS

₸t Thaynes Formation (Early Triassic) Dark gray to brown limestone, siltstone, sandstone, and dolomite. A regional unconformity separates this unit from the underlying Park City Group.

Ppc Park City Group, undivided (late Permian) Light-gray to white limestone with white nodular chert, light-gray dolomite with white nodular chert, bedded chert, phosphatic shale, siltstone, and fine-grained sandstone. This undivided unit is interpreted as a composite of the Kaibab Limestone, Plympton Formation, and Gerster Limestone, which compose the Park City Group in northeastern Nevada (Wardlaw and Collinson, 1978). These units are well-exposed and subdivided in the southeastern East Humboldt Range (Taylor, 1984).

Pu Permian sedimentary rocks, undivided (Permian) Limestone, cherty limestone, sandstone, and limestone conglomerate. Massive bedding and large conglomerate layers, combined with frequent brecciation, commonly hinder bedding observations.

Pp Pequop Formation (early Permian) Comprised of a lower, thin to moderately thick-bedded (up to 50 cm), light to medium-gray limestone with minor, interbedded dolomite and an upper, platy, thin-bedded ($\leq$ 2 cm), purplish-gray silty limestone, calcareous mudstone, and minor dolomite. Fusulinid-rich beds are common, and irregular lenses of dark chert are locally common in the lower unit. Channel-filling debris deposits (debrites) up to 2 m thick and 20 m wide and containing rounded to subangular clasts up to 20 cm diameter of fine, dark gray variably fossiliferous (fusulinids, crinoids, brachiopods) limestone are scattered through the upper part. The contact with underlying Ely Limestone is an unconformity commonly marked by a basal, light tan to light reddish-brown, slope-forming siltstone or fine quartz sandstone varying in thickness from a few m to 20 m. Intraformational folds recognized in the southeastern part of the quadrangle.

Plc Limestone and conglomerate (early Permian) Massive-bedded, medium-gray to dark-gray cherty limestone; chert is commonly gray to black and forms irregular masses to lenticular layers; also light-gray limestone with yellowish-orange chert masses, some massive limestone beds without chert; locally fusulinid-rich limestone; chert- and limestone-clast, calcareous conglomerate and grit, limestone beds intercalated with conglomeratic strata; chert-clasts in conglomeratic rocks are chiefly light colored (white, pale gray, and yellowish tan).

PIPu Ferguson Mountain Formation and Ely Limestone, undivided (Pennsylvanian to early Permian) Undivided light-gray limestone, cherty limestone, and silty limestone mapped in the Wood Hills (e.g., Camilleri, 2010).

IPe Ely Limestone (Pennsylvanian) Light to medium gray, massive to medium limestone separated by thin intervals of argillaceous platy limestone that form bench-and-bluff topography. Beds are comprised of bioclastic limestone containing crinoid, brachiopod, coral, and bryozoan debris. Characteristic irregular lenses and nodules of dark, tan-weathering chert throughout. The change from chert-pebble conglomerate of the Diamond Peak Formation to limestone of the Ely Formation is gradational.

Mdp Diamond Peak Formation (Late Mississippian) Yellow-tan to red subangular to subrounded chert/quartzite conglomerate and tan medium- to fine-grained sandstone. Clasts are up to 10 cm in diameter, and predominantly white, gray, green, red, or black chert and minor quartzite. Matrix is medium- to coarse-grained quartz and chert grains.

The upper Diamond Peak Formation consists of medium gray, micritic, bioclastic limestone with sparse irregular chert nodules. Contact with overlying Ely Limestone is commonly gradational, with interbedded limestone and conglomerate beds. The contact with the underlying Lower Mississippian Chainman Shale is generally poorly exposed but appears gradational, from scattered channel-fill conglomerates in the upper part of the Chainman Shale to more continuous conglomerate beds in the Diamond Peak Formation. This unit may be up to ~300 m thick, as exposed in the Pequop Mountains.

Mdpc Chainman Shale and Diamond Peak Formation, undivided (Mississippian) Tan to light-gray shale, siltstone, and chert-pebble conglomerate.

Mc Chainman Shale (Early Mississippian) Nonresistant, poorly exposed shale, siltstone and fine sandstone, and minor chert-pebble conglomerate. The lower part is black shale with subordinate thin beds of dirty chert-pebble conglomerates and medium- to coarse-grained to gritty, chert-quartz gritstone and an upper part of light gray, fine siltstone and sandstone with subordinate black shale and chert-pebble conglomerate lenses that increase in abundance upwards towards the contact with overlying Diamond Peak Formation. Bedding-parallel faults and internal folds, some isoclinal. Exposures in the southern part of the quadrangle are hornfelsed and more resistant. The basal contact with the Lower Mississippian Joana Limestone is sharp. Apparent structural thickness of as much as 1,000 m may represent tectonic thickening.

Mm Sandstone of Melandco (Early Mississippian) Yellow-brown weathering sandstone and pebble-to-cobble conglomerate.

Mtp Tripon Pass Limestone (Early Mississippian, Kinderhookian) Present only in the southwestern part of the quadrangle, where it consists of gray, medium- to thin-bedded, fine- to medium-grained limestone, commonly with graded beds. Basal beds are thin- to medium-bedded crinoidal coquina limestones (encrinites) that are overlain by light to dark brown, cherty limestones and sandstones. These rocks grade upward into platy to thin- to medium-bedded, fine- to medium-grained limestones that are locally silicified, especially near high-angle faults. Locally becomes sandy, with grains of quartz and chert. Contains interbeds of fissile to platy brown calcareous shale. Contact with underlying Guilmette Formation is a disconformity. Time equivalent to Early Mississippian Joana Limestone. Approximately 270 m thick.

Mj Joana Limestone (Early Mississippian) Present in most of the southern part of the quadrangle, where it consists of light gray limestone marble with encrinite beds and minor chert stringers in the lowermost section. The prominent cliff-forming unit forms a sharp contact with the overlying recessive Early Mississippian Chainman Shale. Approximately 45 m thick. Joana cryptically transforms southward along strike into partly stratigraphically equivalent Tripon Pass Limestone.

Dg Guilmette Formation (Devonian) Mostly consists of gray, medium- to thick-bedded to massive, medium-grained limestone with sparse platy interbeds, dolomite, and sandy limestone that forms prominent cliffs. Locally contains zebra-dolomite beds. Fossiliferous beds contain megascopic stromatoporids, brachiopods, crinoids (encrinites), and corals. Debrite consisting of mostly rounded and flattened clasts of limestone up to 20 cm long that contain variable amounts of rounded quartz grains is prominent in the upper part of the formation in the southern part of the quadrangle. In the southern half of the map, evidence for internal faulting and folding suggest tectonic thickening of the unit. Basal unit (~5 to 25 m in thickness) of yellowish-gray, thin-bedded to platy to argillaceous, *Atrypa nevadana*-bearing limestone that forms a smooth, covered slope in the Pequop Summit quadrangle (Henry and Thorman, 2015) is rarely present in the Independence Valley NE quadrangle, possibly because of bedding-parallel faulting. Pink-gray weathering platy limestone is observed near the base, and a recessive yellowish-gray platy to argillaceous limestone is common in the upper section. Presence of upper Middle Devonian *Stringocephalus* in the upper part of the Simonson Dolomite indicates that the base of the Guilmette Formation cannot be older than uppermost Middle Devonian. Variably 520 m to 650 m thick.

Ds Simonson Dolomite (Devonian) Lower part consists of laminated light-gray to black dolomite and minor gray-green laminated limestone. As many as three thin (0.5- to 2-m-thick) layers of light red-brown-weathering, planar to cross-bedded, siliceous to dolomitic quartzites are present at the base of the unit through much of the area. Upper part consists of interbedded dolomite and limestone, including *Stringocephalus*-bearing biostromes, and probably is equivalent to the Fox Mountain formation of Sandberg et al.

(1997) and Sandberg and Morrow (2009). Ovoid to irregular boudins of dolomite up to 10 m long in foliated limestone are common. The contact between the Simonson Dolomite and the overlying Guilmette Formation is placed at the base of cliff-forming limestone assigned to the Guilmette Formation. Thickness varies from 300 m to 400 m.

DSd Dolostone (Devonian to Silurian) Gray to black, thinly bedded, fine- to medium-grained dolostone and quartz sandstone. The unit consists of undivided Silurian Laketown Dolomite, Early Devonian Sevy Dolomite, and Middle Devonian Simonson Dolostone. This unit is locally exposed as a fault-bounded sliver in southern Clover Hill and Singal Hill, east of the East Humboldt Range.

DSlm Lone Mountain Dolomite (Devonian to Silurian) Mostly light to very light gray, rarely medium gray, massive to faintly bedded dolomite. Approximately 150–180 m thick.

Srm Roberts Mountains Formation (Silurian) Thin-bedded to platy, fine-grained, medium to dark gray limestone and dolomite. Upper part more dolomitic; lower part more limestone. However, relative proportions of limestone and dolomite change gradationally along strike. Locally fossiliferous containing crinoid, brachiopod, and graptolite fragments. Approximately 140 m thick.

Sl Laketown Dolomite (Silurian) Interbedded light to medium gray, fine- to medium-grained dolomite. Lighter and darker intervals range from 15 to 30 m thick. Beds vary from massive to fine to coarsely laminated. Light-colored to grayish-black chert lenses are common. Bioclastic debris and well-preserved crinoids, corals, and brachiopods occur at several horizons. Contact with underlying Fish Haven Dolomite at base of lowest light gray dolomite. Approximately 85 m thick.

SObx Brecciated Laketown Dolomite, Fish Haven Dolomite, and Eureka Quartzite, undivided (Silurian to Ordovician) Brecciated quartzite and dolomite in the Wood Hills.

Ofh Fish Haven Dolomite (Late Ordovician) Dark gray to black, massive to medium- to rarely thinly-bedded, fine-grained dolomite. Basal beds typically contain black to dark gray chert lenses. Bioclastic debris, especially of crinoids, is common.

Oe Eureka Quartzite (Middle Ordovician) Vitreous, mostly white to lesser medium gray to purple quartzite composed of medium-grained, rounded quartz grains that generally are frosted. The unit is generally intact in the map area, although it is variable brecciated in the Independence Valley NE quadrangle. The unit forms prominent light-colored cliffs of medium-bedded, mostly planar to less commonly cross-bedded rock; crossbeds typically expressed by light blue color bands, where strongly silicified or by selective weathering of carbonate near base or top of formation. Basal and upper quartzite beds are generally darker than interior beds, ranging to medium to dark gray and purple. Thin sections from a sample collected from the prominent Oe cliff band on the western flank of the range shows quartz grains with shape-preferred orientations (SPO) but no lattice-preferred orientation (LPO). Quartz grain boundaries are comprised of small bulges and small recrystallized grains, suggesting bulging recrystallization. A slightly polygonized texture and faint presence of subgrains suggests minor subgrain rotation recrystallization. Undulose extinction is common. These characteristics suggest that these rocks experienced temperatures of 300–400°C, which is corroborated by Raman spectroscopy on carbonaceous material (RSCM), calcite-dolomite (CD), and conodont color alteration index (CAI) thermometry (Howland, 2016; Zuza et al., 2019).

Pogonip Group

The Pogonip Group includes the following formations and informal members:

Opl Lehman Formation (Early Ordovician) Medium gray-blue, fine-grained platy to medium-bedded limestone with thin, tan, argillaceous interbeds and irregular bodies, possibly burrows. Locally contains abundant leperditia (small, pea-shaped ostracod). Grades upward into dark-gray dolomite (Crystal Peak Dolomite, not mapped separately here) and sandy dolomite of Eureka Quartzite. Approximately 150 m to 250 m thick.

Kanosh Formation

The Kanosh Formation includes the following informal units: upper shale (Kanosh Shale), middle limestone (Kanosh limestone), and basal quartzite (Kanosh quartzite).

Opks Kanosh Shale (Early Ordovician) Yellowish-brown, olive, gray to black, fissile shale with intercalated platy argillaceous limestone similar to Lehman Limestone. Forms covered slopes between bounding units and upper and lower contacts are covered. Limestone layers commonly contain abundant leperditia. Poorly exposed, but probably 20–30 m thick.

Opkl Kanosh limestone (Early Ordovician) Medium gray-blue, fine-grained limestone with thin, tan, argillaceous interbeds, similar to the Lehman Limestone. Approximately 160 m thick.

Opkq Kanosh quartzite (Early Ordovician) Cross- to planar-bedded, medium-grained, light brown to red-brown weathering, well-cemented quartzite with minor, commonly leached carbonate matrix. Locally absent between the House and Kanosh limestones, probably due to boudinage development. Etching of carbonate matrix due to weathering makes characteristic pitted surface and accentuates crossbeds, which distinguishes it from Eureka Quartzite. Approximately 8 m thick.

Opk Kanosh Formation, undivided (Early Ordovician) Undivided limestone, quartzite, and shale.

Oplk Kanosh Formation and Lehman Formation, undivided (Early Ordovician) Undivided limestone, quartzite, and shale. The Kanosh Shale and Kanosh Quartzite are marker horizons typically used to differentiate stratigraphic position between the Kanosh and Lehman Formations, but in some cases across the map, this is not possible.

Oph House Limestone (Early Ordovician) Medium gray, fine-grained platy to medium-bedded limestone with argillaceous bedding planes and irregular bodies, possibly burrows. More shale and argillite component than Lehman Formation. Approximately 400 m thick.

METAMORPHOSED PALEOZOIC AND PROTEROZOIC ROCKS

Msq Schist and quartzite paragneiss (Mississippian?) Dark rust gray to brown micaceous feldspathic quartzite and metaconglomerate, quartzofeldspathic schist, pelitic schist, and minor calcareous paragneiss. Minor calc-silicate and calcareous paragneiss comprise the lower part of the unit. Unit is similar to the MDgs unit. Detrital zircon analyses reveal age spectra that are dissimilar from McCoy Creek Group rocks (e.g., Gehrels and Pecha, 2014) and most similar to a mylonitic Diamond Peak Formation sample analyzed from the Secret Valley quadrangle to the south (Zuza et al., 2021a, 2022). These results strengthen the correlation of the Msq unit with Mississippian Diamond Peak Formation and Chainman Shale, although we acknowledge that Mississippian clastic rocks do not yield unique detrital zircon spectra.

MDgs Graphitic schist and calcareous paragneiss (Mississippian to Late Devonian?) Graphitic, micaceous quartzite and quartzofeldspathic schist, pelitic schist, and calc-silicate paragneiss that weathers to a rusty brown. Observed within fold nappes in the East Humboldt Range. Metamorphic minerals include garnet, sillimanite, and/or kyanite (McGrew et al., 2000; Hallett and Spear, 2014). The unit likely correlates with the Mississippian Chainman Shale or Devonian–Mississippian Pilot Shale, including underlying Mississippian Tripon Pass or Joana Limestones. The unit has variable thicknesses from 1 m to 25 m.

MꞒmu Marble, undivided (Mississippian to Cambrian) Impure calcite, dolomite, calc-silicate marble, schist, paragneiss and quartzite. Marbles have heterogenous color and appearance, including pale white-gray coarse-grained massive layers, fine-grained gray-blue banded layers, green-gray to gray impure silty marble, and coarse massive blue-gray layers. Commonly muscovite-rich with graphite and tremolite. Calc-silicate with diopside and garnet observed along margins when unit is intruded by TKlg and Tqd. Contact with the underlying ꞒZpm or ꞒZpmi is sharp, marked by the presence of pure quartzite beds and disappearance of marbles.

Dgm Guilmette Formation, metamorphosed (Devonian) Fine-grained blue-gray to white calcite marble with white color bands, recrystallized fossils, and graphite. Some dolomite layers. Commonly in contact with OꞒmi or OꞒm, without intervening Oe, suggests normal-sense structural omission.

DOd Dolomite and marble (Devonian to Ordovician) White to blue-gray, fine-grained, massive dolomite marble with sparse graphite and tremolite. Subordinate marbles interbedded with mostly dolomite. Distinguished from MꞒmu by abundance of dolomite.

Oem Metamorphosed Eureka Quartzite (Ordovician) Finely recrystallized mylonitized white quartzite with foliation defined by minor muscovite and graphite bands. Outcrops are commonly discontinuously scattered within Paleozoic marbles or shales, potentially as a result of boudinage during Cenozoic extension. Exposed thickness range between ~1 and 10 meters.

OꞒnp Notch Peak Formation (Early Ordovician to Late Cambrian) Predominantly light to medium gray dolomitic marble with local thick interbeds of blue and white limestone. Dolomitic marble is massive to banded light gray or tan to medium gray or tan. 2- to 5-cm-thick lenses and nodules of medium-gray chert are sparse to locally abundant, especially near the top of the formation. Limestone is well-bedded with tan, silty layers, similar to limestone of the Pogonip Group. Zebra dolomite makes a few beds in the upper part. Dolomite commonly forms ovoid to irregular boudins up to 10–15 m in diameter in flowed limestone. Contact with underlying Dunderberg Shale is gradational; dolomite or limestone are interbedded with phyllite and schist. No measured thickness in the map area, but Smith et al. (2013) show 380 m thickness and Camilleri (2010) suggest a range from 350 m to 600 m.

O€m Impure calcite marble (Ordovician to Cambrian) Impure calcite, dolomite, and calc-silicate marble with variable amounts of tan-to-orange silty interbeds. Marbles have heterogenous color and appearance, including pale white-gray coarse-grained massive layers, fine-grained gray-blue banded layers, green-gray to gray impure silty marble, and coarse massive blue-gray layers. Commonly muscovite-rich with graphite and tremolite. Calc-silicate with diopside and garnet observed along margins when unit is intruded by TKlg and Tqd. Lowermost part of unit includes highly folded siliciclastic and impure marble layers.

Contact with the underlying €Zpm or €Zpmi is sharp, marked by the presence of pure quartzite beds and disappearance of marbles. Some marbles near, or below, this interpreted contact may be Zmm marbles, which are commonly thinner (mostly <5 m thick) and surrounded by quartzite and pelite.

O€mi Intruded impure calcite marble (Ordovician to Cambrian) Micaceous feldspathic quartzite with subordinate pelitic schist, and locally with calc-silicate gneiss and rare para-amphibolite. Upper unit commonly consists of a relatively pure quartzite interpreted to correlate with the Prospect Mountain Quartzite. Rare intrusions compared with mapped €Zpmi.

€d Dunderberg Shale (Cambrian) Recessive weathering, poorly exposed unit consisting of green and black shale metamorphosed to phyllite and schist, especially in the footwall of the Independence thrust, commonly with fine porphyroblasts. Contains numerous thin (≤10 cm) micaceous limestone interbeds. Muscovite is parallel to foliation and biotite is oblique to foliation. Sharp contact with underlying Oasis Formation. Approximately 50–60 m thick in the map area.

€o Oasis Formation (Cambrian) Cliff-forming white, light gray, and blue-gray medium- to thick-bedded limestone and dolomite marble. White and light gray limestone and dolomite make up the top and bottom of the unit, and blue-gray limestones, similar in appearance to Clifside Limestone, make up the middle of the formation. Tan silt beds appear similar to those in Pogonip limestones but are commonly more sheared. The occurrence of thin-bedded silty limestone or shale marks the contacts with overlying and underlying Dunderburg Shale and Shafter Formation, respectively. Approximately 200 m thick.

€s Shafter Formation (Cambrian) Thinly bedded gray to blue limestone marble with silty orange to gray interbeds commonly metamorphosed to phyllite or schist. Unit is recessive, with areas weathered to dark brown. Approximately 130 m thick in the map area.

€dl Decoy Limestone (Cambrian) Distinctive cliff-forming tan-gray recrystallized dolomite or light blue-gray recrystallized limestone with silty limestone interbeds. Can resemble Clifside Limestone where not dolomitized or deformed. Contact with underlying recessive Morgan Pass Formation occurs with the appearance of silty limestone. Variably 30 m to 60 m thick.

€mp Morgan Pass Formation (Cambrian) Recessive weathering shale and platy blue limestone. Metamorphosed to micaceous schist and marble. Muscovite is parallel to foliation and biotite, where observed, is oblique to foliation. The contact with the underlying Clifside Limestone is sharp at the base of the lowest shale or silty limestone above the distinct cliff-forming gray Clifside Limestone. Approximately 120 m thick in the map area.

€cl Clifside Limestone (Cambrian) Wavy-foliated, light gray-blue calcareous marble, commonly with coarse muscovite, with gray or orange-brown silty layers and locally, abundant crinoids and other strongly recrystallized fossils. A minor brown silty limestone section, metamorphosed to muscovite-biotite schist, near the middle of the Clifside Limestone is recessive and poorly exposed. Thickness varies substantially in the map area, from 100 m to 200 m.

€t Toano Limestone (Cambrian) Foliated, dark grayish green micaceous marble with much less phyllite and tremolite schist than in underlying Killian Springs Formation. Protoliths were likely thin-bedded limestone and silty limestone. Some beds are chaotically folded, probably due to slumping and soft-sediment deformation because the enveloping layers are not deformed. The contact with the overlying Clifside Limestone is placed at the distinct color and lithologic change, Toano Limestone being darker green and more micaceous. Approximately 170 m thick in the map area.

Ꞓks Killian Springs Formation (Cambrian) Black to dark greenish gray micaceous marble, phyllite, and biotite-muscovite or hornblende schist with tremolite-bearing layers. Protoliths were likely siltstone, calcareous siltstone and thin-bedded limestone. Contact with underlying Cambrian Prospect Mountain Quartzite is sharp. Approximately 170 m thick in the northern Pequop Mountains.

Ꞓu Metamorphosed Dunderberg Shale, Oasis Formation, Shafter Formation, Decoy Limestone, Morgan Pass Formation, undivided (Cambrian) Schist and light-gray to white to cream-colored calcite marble and micaceous calcite marble in uppermost part of unit (= Dunderberg Shale) and underlying light-gray to gray-green to light-gray-blue calcite marble and micaceous calcite marble with minor tan dolomite marble.

ꞒZpm Metamorphosed Prospect Mountain Quartzite (Cambrian to Neoproterozoic protolith age) and McCoy Creek Group (Neoproterozoic protolith age), undivided Micaceous feldspathic quartzite with subordinate pelitic schist, and locally with calc-silicate gneiss and rare para-amphibolite. Upper unit commonly consists of a relatively pure quartzite interpreted to correlate with the Prospect Mountain Quartzite. Stratigraphically deeper rocks consist of alternating quartzite and pelitic layers of the McCoy Creek Group. At deep structural levels, this unit may be extensively intruded by leucogranite, quartz diorite, and monzogranite. Commonly migmatitic, with pelitic rocks hosting a higher percentage of leucosome than quartzitic rocks.

Zmu Metamorphosed McCoy Creek Group, undivided (Neoproterozoic) Micaceous quartzite, feldspathic quartzite, garnet-biotite schist (±sillimanite) with lesser marble, calc-silicate, and rare amphibolite. Extensively intruded by leucogranite, monzogranite, and quartz diorite. Divided from ꞒZpmi or ꞒZpm based on occurrence of extensive pelitic layers or interlayered coarse white-gray Zmm marbles.

Zmum Migmatitic McCoy Creek Group, undivided (Neoproterozoic) Migmatitic McCoy Creek Group paragneiss, commonly containing >50% leucogranitic rock. Transition with structurally higher Zmu is gradiational over 50–100 m.

Zmm McCoy Creek Group marble (Neoproterozoic) Discontinuous coarse-grained, graphite-bearing, white-gray calcite marble. Forms continuous and discontinuous layers that range in thickness from ~1 m to ~100 m (mostly <5 m). Marble margins are sometimes replaced by calc-silicate assemblages with diopside, grossular garnet, and actinolite. Divided from OꞒm and OꞒmi because Zmm layers are commonly thin, always white-gray in color, and surrounded by quartzite and pelite.

ZXpg Paragneiss and amphibolite (Neoproterozoic to Paleoproterozoic) Impure micaceous metaquartzite, biotite-sillimanite schist, and paragneiss. Boudins of meter-scale amphibolite and garnet amphibolite interpreted as metamorphosed small mafic intrusions. Migmatization is widespread with more pelitic components commonly hosting large volumes of leucosome, especially at deeper structural levels on the lower limb of the Winchell Lake fold. Detrital zircon geochronology of most samples defines a strong minimum provenance of Grenville age (800–1,250 Ma) supporting correlation with the McCoy Creek Group, but a sample of fuchsitic quartzite shows a much older minimum age provenance of ~2,400 Ma suggesting that the unit may locally include Paleoproterozoic rocks (Premo et al., 2014).

XWpg Paragneiss, undivided (Paleoproterozoic to Neoarchean?) Micaceous quartzofeldspathic paragneiss, metaquartzite, and biotite (-sillimanite) schist with voluminous leucogranite intrusions. Intruded by meter-scale amphibolite and garnet amphibolite. Detrital zircon geochronology defines one provenance population of ~2,550 Ma and another of ~2,450 Ma (Premo et al., 2014). These dates suggest the unit could be as old as Neoarchean. Metamorphic zircon overgrowths at ~1,770 Ma require that original deposition occurred no later than Paleoproterozoic (Premo et al., 2014).

XWog Orthogneiss (Paleoproterozoic to Neoarchean) Gray, medium-to-coarse-grained quartzofeldspathic gneiss. Commonly migmatitic with local amphibolite boudins. Premo et al. (2014) reported an Archean SHRIMP U-Pb zircon age of 2,449 ± 3 Ma that suggests this unit may reflect Neoarchean North American basement. Alternatively, this unit may reflect a complex overprinting metamorphism of a granite melt that incorporated inherited Archean detrital grains (Premo et al., 2008).

ACKNOWLEDGMENTS

Research and map compilation supported by the U.S. Geological Survey, National Cooperative Geologic Mapping Program, under USGS award numbers G21AC10873, 2021 and G22AC00578, 2022. Previously, USGS support for maps synthesized in this compilation include G14AC00237, G15AC00240, G16AC00186, G17AC00212, G18AC00198, G19AC00383, and G20AC00390. The views and conclusions contained in this document are those of the authors and should not be interpreted as necessarily representing the official policies, either expressed or implied, of the U.S. Government. We thank the geologists who contributed to the mapping in this synthesis, including Art Snoke, Allen McGrew, Phyllis Camilleri, Karri Siccard, Hugh Hurlow, Keith Howard, and Chuck Thorman. We appreciate support provided for production from the Geological Society of Nevada.

REFERENCES

Barnes, C.G., Burton, B.R., Burling, T.C., Wright, J.E., and Karlsson, H.R., 2001, Petrology and geochemistry of the late Eocene Harrison Pass pluton, Ruby Mountains core complex, northeastern Nevada: Journal of Petrology, v. 42, no. 5, p. 901–929.

Batum, M.A., 1999, Petrology of Late Cretaceous and Cenozoic grantic rocks, East Humboldt Range, northeastern Nevada, Texas Tech University: Ph.D. dissertation.

Bedell, R., Struhsacker, E., Craig, L., Miller, M., Coolbaugh, M., Smith, J., and Parratt, R., 2010, The Pequop mining district, Elko County, Nevada—an evolving new gold district: Society of Economic Geologists Special Publication 15, p. 29–56.

Bonnichsen, B., Leeman, W.P., Honjo, N., McIntosh, W.C., and Godchaux, M.M., 2008, Miocene silicic volcanism in southwestern Idaho—geochronology, geochemistry, and evolution of the central Snake River Plain: Bulletin of Volcanology, v. 70, no. 3, p. 315–342.

Brooks, W.E., Thorman, W.E., and Snee, L.W., 1995a, The ^{40}Ar/^{39}Ar ages and tectonic setting of the middle Eocene northeast Nevada volcanic field: Journal of Geophysical Research, v. 100, p. 10,403–10,416.

Brooks, W.E., Thorman, W.E., Snee, L.W., Nutt, C.W., Potter, C.J., and Dubiel, R.F., 1995b, Summary of chemical analyses and ^{40}Ar/^{39}Ar-spectra data for often Eocene volcanic rocks from the central part of the northeast Nevada volcanic field: U.S. Geological Survey Bulletin 1988-K, p. K1–K33.

Brueseke, M.E., Hart, W.K., and Heizler, M.T., 2008, Diverse mid-Miocene silicic volcanism associated with the Yellowstone–Newberry thermal anomaly: Bulletin of Volcanology, v. 70, no. 3, p. 343–360.

Brueseke, M.E., Callicoat, J.S., Hames, W., and Larson, P.B., 2014, Mid-Miocene rhyolite volcanism in northeastern Nevada—the Jarbidge Rhyolite and its relationship to the Cenozoic evolution of the northern Great Basin (USA): Geological Society of America Bulletin, v. 126, p. 1,047–1,067.

Camilleri, P., 2010, Geologic map of the Wood Hills, Elko County, Nevada: Nevada Bureau of Mines and Geology Map 172, scale 1:48,000, 16 p.

Castor, S.B., Boden, D.R., Henry, C.D., Cline, J.S., Hofstra, A.H., McIntosh, W.C., Tosdal, R.M., Wooden, J.P., 2003, Geology of the Eocene Tuscarora volcanic-hosted, epithermal precious metal district, Elko County, Nevada: Economic Geology, v. 98, p. 339–366.

Christiansen, R.L., 2001, The Quaternary and Pliocene Yellowstone Plateau volcanic field of Wyoming, Idaho, and Montana: US Geological Survey Professional Paper 729-G, 145 p.

Coats, R.R., 1987, Geology of Elko County, Nevada: Nevada Bureau of Mines and Geology Bulletin 101, scale 1:250,000, 112 p.

Colgan, J.P., and Henry, C.D., 2009, Rapid middle Miocene collapse of the Sevier orogenic plateau in north-central Nevada: International Geology Review, v. 51, p. 920–961, doi:10.1080/00206810903056731.

Colgan, J.P., Howard, K.A., Fleck, R.J., and Wooden, J.L., 2010, Rapid middle Miocene extension and unroofing of the southern Ruby Mountains, Nevada: Tectonics, v. 29, p. TC6022, doi:10.1029/2009TC002655.

Dallmeyer, R.D., Snoke, A.W., and McKee, E.H., 1986, The Mesozoic-Cenozoic tectonothermal evolution of the Ruby Mountains, East Humboldt Range, Nevada—a Cordilleran metamorphic core complex: Tectonics, v. 5, no. 6, p. 931–954.

Dee, S., and Ressel, M.W., 2016, Preliminary geologic map of the Herder Creek quadrangle, Elko County, Nevada: Nevada Bureau of Mines and Geology Open-File Report 2016-05, scale 1:24,000, 5 p.

Dee, S., Dering, G.M., and Henry, C.D., 2015, Preliminary geologic map of the Heelfly Creek quadrangle and adjacent parts of the Tent Mountain, Soldier Peak, and Secret Valley quadrangles, Elko County, Nevada: Nevada Bureau of Mines and Geology Open-File Report 2015-04, scale 1:24,000, 5 p.

Gehrels, G., and Pecha, M., 2014, Detrital zircon U-Pb geochronology and Hf isotope geochemistry of Paleozoic and Triassic passive margin strata of western North America: Geosphere, v. 10, no. 1, p. 49–65.

Hallett, B.W., and Spear, F.S., 2014, The P–T history of anatectic pelites of the northern East Humboldt Range, Nevada—evidence for tectonic loading, decompression, and anatexis: Journal of Petrology, v. 55, no. 1, p. 3–36.

Hallett, B.W., and Spear, F.S., 2015, Monazite, zircon, and garnet growth in migmatitic pelites as a record of metamorphism and partial melting in the East Humboldt Range, Nevada: American Mineralogist, v. 100, no. 4, p. 951–972.

Henry, C.D., 2008, Ash-flow tuffs and paleovalleys in northeastern Nevada—implications for Eocene paleogeography and extension in the Sevier hinterland, northern Great Basin: Geosphere, v. 4, p. 1–35.

Henry, C.D., and Boden, D.R., 1998, Geologic map of the Mount Blitzen quadrangle, Elko County, northeastern Nevada: Nevada Bureau of Mines and Geology Map 110, 1:24,000, 20 p.

Henry, C.D., and Thorman, C.H., 2011, Geologic map of the Wells area, Elko County, Nevada *in* dePolo, C.M., and LaPointe, D.D., editors, The 21 February 2008 M_W 6.0 Wells, Nevada Earthquake—a compendium of earthquake-related investigations prepared by the University of Nevada, Reno: Nevada Bureau of Mines and Geology Special Publication 36.

Henry, C.D., and Thorman, C.H., 2015, Preliminary geologic map of the Pequop Summit quadrangle, Elko County, Nevada: Nevada Bureau of Mines and Geology Open-File Report 2015-08, scale 1:24,000, 12 p.

Henry, C.D., McGrew, A.J., Colgan, J.P., Snoke, A.W., and Brueseke, M.E., 2011, Timing, distribution, amount, and style of Cenozoic extension in the northern Great Basin, *in* Lee, J., and Evans, J.P., editors, Geologic field trips to the Basin and Range, Rocky Mountains, Snake River Plain, and Terranes of the U.S. Cordillera: Geological Society of America Field Guide, v. 21, p. 27–66.

Henry, C.D., Hinz, N.H., Faulds, J.E., Colgan, J.P., John, D.A., Brooks, E.R., Cassel, E.J., Garside, L.J., Davis, D.A., and Castor, S.B., 2012, Eocene-Early Miocene paleotopography of the Sierra Nevada–Great Basin–Nevadaplano based on widespread ash-flow tuffs and paleovalleys: Geosphere, v. 8, p. 1–27.

Henry, C.D., Castor, S.B., Starkel, W.A., Ellis, B.S., Wolff, J.A., Laravie, J.A., and Heizler, M.T., 2017, Geology and evolution of the McDermitt caldera, northern Nevada and southeastern Oregon, western USA. Geosphere, 13(4), 1066–1112.

Howland, C., 2016, High thermal gradient in the upper plate of a core complex, determined by calcite-dolomite and RSCM thermometry, Pequop Mountains, NV (B.S. Honors Thesis): Schenectady, New York, Union College, 135 p.

Hudec, M.R., 1990, The structural and thermal evolution of the central Ruby Mountains, Elko County, Nevada: University of Wyoming, Laramie, Ph.D. dissertation, 272 p.

Hudec, M.R., 1992, Mesozoic structural and metamorphic history of the central Ruby Mountains metamorphic core complex, Nevada: Geological Society of America Bulletin, v. 104, no. 9, p. 1,086–1,100.

Kuiper, K.F., Deino, A., Hilgen, F.J., Krijgsman, W., Renne, P.R., and Wijbrans, A.J., 2008, Synchronizing rock clocks of Earth history: Science, v. 320, no. 5875, p. 500–504.

Laabs, B.J., Licciardi, J.M., Leonard, E.M., Munroe, J.S., and Marchetti, D.W., 2020, Updated cosmogenic chronologies of Pleistocene mountain glaciation in the western United States and associated paleoclimate inferences: Quaternary Science Reviews, v. 242, 36 p.

Lanphere, M.A., Champion, D.E., Christiansen, R.L., Izett, G.A., and Obradovich, J.D., 2002, Revised ages for tuffs of the Yellowstone Plateau volcanic field—assignment of the Huckleberry Ridge Tuff to a new geomagnetic polarity event: Geological Society of America Bulletin, v. 114, no. 5, p. 559–568.

McGrew, A.J., 2018, Geologic map of the Humboldt Peak quadrangle, Elko County, Nevada: Nevada Bureau of Mines and Geology Map 186, scale 1:24,000, 23 p.

McGrew, A.J., and Snoke, A.W., 2015, Geologic map of the Welcome quadrangle and an adjacent part of the Wells quadrangle, Elko County, Nevada: Nevada Bureau of Mines and Geology Map 184, scale 1:24,000, 40 p.

McGrew, A.J., Peters, M.T., and Wright, J.E., 2000, Thermobarometric constraints on the tectonothermal evolution of the East Humboldt Range metamorphic core complex, Nevada: Geological Society of America Bulletin, v. 112, no. 1, p. 45–60.

McIntosh, W.C., Heizler, M., Peters, L., and Esser, R., 2003, $^{40}Ar/^{39}Ar$ geochronology at the New Mexico Bureau of Geology and Mineral Resources: New Mexico Bureau of Geology and Mineral Resources Open-File Report OF-AR-1, 10 p.

Min, K., Mundil, R., Renne, P.R., and Ludwig, K.R., 2000, A test for systematic errors in $^{40}Ar/^{39}Ar$ geochronology through comparison with U/Pb analysis of a 1.1-Ga rhyolite: Geochimica et Cosmochimica Acta, v. 64, no. 1, p. 73–98.

Mueller, K.J., 1992, Tertiary basin development and exhuation of the northern East Humboldt–Wood Hills metamorphic complex, Elko County, Nevada: University of Wyoming, Laramie, Ph.D. dissertation, 205 p.

Mueller, K.J., Cerveny, P.K., Perkins, M.E., and Snee, L.W., 1999, Chronology of polyphase extension in the Windermere Hills, northeast Nevada: Geological Society of America Bulletin, v. 111, p. 11–27.

Munroe, J.S., and Laabs, B.J., 2013, Temporal correspondence between pluvial lake highstands in the southwestern US and Heinrich event 1: Journal of Quaternary Science, v. 28, no. 1, p. 49–58.

Palmer, H.C., and MacDonald, W.D., 2002, The northeast Nevada volcanic field—magnetic properties and source implications: Journal of Geophysical Research, v. 107, doi: 1029/2001JB000690.

Premo, W.R., Castiñeiras, P., and Wooden, J.L., 2008, SHRIMP-RG U-Pb isotopic systematics of zircon from the Angel Lake orthogneiss, East Humboldt Range, Nevada—is this really Archean crust?. Geosphere, v. 4, no. 6, 963–975.

Premo, W.R., Moscati, R.J., McGrew, A.J., and Snoke, A.W., 2014, New U-Pb geochronology of Precambrian paragneisses and late Phanerozoic orthogneisses of the Angel Lake–Lizzies Basin region of the East Humboldt Range, northeastern Nevada—a comparison with the thermal chronology at Lamoille Canyon in the adjacent Ruby Mountains: Geological Society of America Abstracts with Programs, v. 46, no. 5, p. 33.

Reheis, M., 1999, Highest pluvial-lake shorelines and Pleistocene climate of the western Great Basin: Quaternary Research, v. 52, no. 2, p. 196–205.

Sandberg, C., and Morrow, J.R., 2009, Recognition of Fox Mountain Formation solves enigmatic Devonian stratigraphy in central and northern Utah: Geological Society of America Abstracts with Programs, v. 41, no. 6, p. 15.

Sandberg, C.A., Morrow, J.R., and Warme, J.E., 1997, Late Devonian Alamo impact event, global Kellwasser events, and major eustatic events, eastern Great Basin, Nevada and Utah: Brigham Young University Geology Studies, v. 42, pt. 1, p. 129–160.

Sharp, R.P., 1938, Pleistocene glaciation in the Ruby–East Humboldt Range, northeastern Nevada: Journal of Geomorphology, v. 1, p. 296–323.

Sharp, R.P., 1940, Geomorphology of the Ruby–East Humboldt Range, Nevada: Bulletin of the Geological Society of America, v. 51, no. 3, p. 337–371.

Sicard, K.R., and Snoke, A.W., 2020, Geologic map of the Gordon Creek quadrangle, Elko County, Nevada: Nevada Bureau of Mines and Geology Map 188, scale 1:24,000, 28 p.

Smith, M.T., Rhys, D., Ross, K., Lee, C., and Gray, J.N., 2013, The Long Canyon deposit—anatomy of a new off-trend sedimentary rock-hosted gold discovery in northeastern Nevada: Economic Geology, v. 108, no. 5, p. 1,119-1,145.

Snoke, A.W., Howard, K.A., and Dee, S., 2021, Geologic map of the Secret Valley quadrangle Elko County, Nevada: Nevada Bureau of Mines and Geology Map 189, scale 1:24,000, 21 p.

Snoke, A.W., Howard, K.A., and Dee, S., 2022, Geologic map of the Soldier Peak quadrangle, Elko County, Nevada: Nevada Bureau of Mines and Geology Map 191, scale 1:24,000, 31 p.

Snoke, A.W., McGrew, A.J., Valasek, P.A., and Smithson, S.B., 1990, A crustal cross-section for a terrain of superimposed shortening and extension—Ruby Mountains–East Humboldt Range metamorphic core complex, Nevada, *in* Salisbury, M.H., and Fountain, D.M., editors, Exposed cross sections of the continental crust: The Netherlands, Kluwer Academic Publishers, p. 103–135.

Steiger, R.H., and Jäger, E., 1977, Subcommission on geochronology—convention on the use of decay constants in geo- and cosmochronology: Earth and Planetary Science Letters, v. 36, no. 3, p. 359–362.

Taylor, G.K., 1984, Stratigraphy, metamorphism, and structure of the southeastern East Humboldt Range, Elko County, Nevada: University of South Carolina, M.S. thesis, 148 p.

Thorman, C.H., 1970, Metamorphosed and nonmetamorphosed Paleozoic rocks in the Wood Hills and Pequop Mountains, northeast Nevada: Geological Society of America Bulletin, v. 81, no. 8, p. 2,417–2,448.

Thorman, C.H., Brooks, W.E., Ketner, K.B., and Dubiel, R.F., 2003, Preliminary geologic map of the Oxley Peak area, Elko County, Nevada: Nevada Bureau of Mines and Geology Open-File Report 2003-04, 1:24,000.

Vlaha, D.R., and Zuza, A.V., 2022, Geologic map of the western half of the Independence Valley SE quadrangle, Elko County, Nevada: EDMAP Final Map, scale 1:24,000, 10 p., https://doi.org/10.13140/RG.2.2.36716.58244.

Wallace, A.R., Perkins, M.E., and Fleck, R.J., 2008, Late Cenozoic paleogeographic evolution of northeastern Nevada—evidence from the sedimentary basins: Geosphere, v. 4, p. 36–74, doi:10.1130/GES00114.1.

Wardlaw, B.R., and Collinson, J.W., 1978, Stratigraphic relations of Park City Group (Permian) in eastern Nevada and western Utah: AAPG Bulletin, v. 62, no. 7, p. 1,171–1,184.

Wesnousky, S.G., and Willoughby, C.H., 2003, Neotectonic note—the Ruby–East Humboldt Range, northeastern Nevada: Bulletin of the Seismological Society of America, v. 93, no. 3, p. 1,345–1,354.

Wright, J.E., and Snoke, A.W., 1993, Tertiary magmatism and mylonitization in the Ruby–East Humboldt metamorphic core complex, northeastern Nevada—U-Pb geochronology and Sr, Nd, and Pb isotope geochemistry: Geological Society of America Bulletin, v. 105, no. 7, p. 935–952.

Zuza, A.V., and Dee, S., 2023, Decoupled Oligocene mylonitic shearing and Miocene detachment faulting in the East Humboldt Range metamorphic core complex, northeast Nevada, USA: Geosphere, v. 19, no. 5, p. 1318–1347.

Zuza, A.V., Henry, C.D., Ressel, M.W., Thorman, C.H., Dee, S., and Blackmon, J.E., 2018, Preliminary geologic map of the Independence Valley NE quadrangle, Elko County, Nevada: Nevada Bureau of Mines and Geology Open-File Report 2018-04, scale 1:24,000, 12 p.

Zuza, A.V., Dee, S., Henry, C.D., Ressel, M.W., and Thorman, C.H., 2019, Geologic map of the Independence Valley NW quadrangle, Elko County, Nevada: Nevada Bureau of Mines and Geology Open-File Report 2019-03, scale 1:24,000, 18 p.

Zuza, A.V., Thorman, C.H., Henry, C.D., Levy, D.A., Dee, S., Long, S.P., Sandberg, C.A., and Soignard, E., 2020, Pulsed Mesozoic deformation in the Cordilleran hinterland and evolution of the Nevadaplano: Insights from the Pequop Mountains, NE Nevada: Lithosphere, v. 1.

Zuza, A.V., Dee, S., Hurlow, H.A., Snoke, A.W., and Laabs, B.J., 2021a, Geologic map of the Tent Mountain quadrangle, Elko County, Nevada: Nevada Bureau of Mines and Geology Open-File Report 2021-03, 1:24,000 scale, 26 p.

Zuza, A.V., Henry, C.D., Dee, S., Thorman, C.H., and Heizler, M.T., 2021b, Jurassic–Cenozoic tectonics of the Pequop Mountains, NE Nevada, in the North American Cordillera hinterland: Geosphere, v. 17, no. 6, p. 2,078–2,122.

Zuza, A.V., Levy, D.A., Dee, S., DesOrmeau, J.W., Cheng, F., and Li, X., 2022, Structural architecture and attenuation of the ductile lower plate of the Ruby Mountain–East Humboldt Range metamorphic core complex, Northeast Nevada: Tectonics, v. 41, no. 8, 38 p.

Table 1. Single crystal $^{40}Ar/^{39}Ar$ analyses from volcanic and volcaniclastic rocks in the Ruby Mountains–East Humboldt Range–Pequop Mountains map compilation, Nevada.

Sample	Map Unit	Rock Type	Location, quad	Material	Ages (Ma)[1]		K/Ca	±2s	n[2]	Notes	Latitude	Longitude	Source
					Weighted mean	±2s							
SD14044	QTa	tephra in Quaternary deposits	I-80	sanidine	2.0	0.10	23.0	7.8	13/19		41.08357	-115.26774	This study
H21-SP44	QTa	tephra in Quaternary deposits	Soldier Peak	sanidine	2.35	0.07	47.1	48.8	13/35	Huckleberry Ridge from geochemical correlation	40.86221	-115.36323	This study
H15-43	**Th**	reworked tephra in Ts	Herder Creek	plagioclase	<5.15	1.82	0.1	0.1	6/26	maximum depositional age; young population of 6	41.01016	-115.21591	This study
GD14-100	**Th**	tephra in Ts	Heelfly Creek	anorthoclase	8.30	0.20	8.5	7.8	11		40.91263	-115.29115	This study
GD14-113	**Th**	tephra in Ts	Heelfly Creek	plagioclase	10.30	0.13			15/19	1 sanidine, 14 plagioclase	40.9469	-115.26526	This study
H14-97	**Th**	reworked tephra in Ts	Heelfly Creek	sanidine	≤12.353	0.01	24.6		1/20	maximum depositional age; youngest sanidine. 4 @ 22.89 Ma probably Pahranagat Tuff	40.88668	-115.30011	This study
GD14-116B	**Th**	tephra in Ts	Heelfly Creek	anorthoclase	15.77	0.02	6.0	4.6	15/20		40.95184	-115.24963	This study
H14-98	**Th**	reworked tephra in Ts	Heelfly Creek	sanidine	<22.7	0.3	27.4	18.7	1/12	maximum depositional age; youngest sanidine	40.88547	-115.29859	This study
H15-42	**Th**	reworked tephra in Ts	Herder Creek	sanidine	<23.27	0.02	20.5	0.3	1/24	youngest sanidine grain	41.00875	-115.21871	This study
H14-52	Tjrc	Jarbidge Rhyolite lava	Tent Mtn	anorthoclase	15.35	0.01	9.6	5.2	19/21		40.9517	-115.24716	This study
H14-54	Tjrf	Jarbidge Rhyolite lava	Secret Valley	anorthoclase	15.37	0.04	9.0	1.9	24/25		40.86918	-115.24614	This study
H23-W373	Th_3	primary pyroclastic-fall deposit, good sanidine, possibly very minor quartz	Welcome, upper Clover Creek sequence	sanidine	10.89	0.03	14.5	1.6	4/25	CPT XIII	41.119177	-115.00165	This study
H23-W377	Th_3	primary pyroclastic-fall deposit, fine-grained, some quartz, plag? Apatite FT from early 90s = 8 ± ~2 Ma	Welcome, upper Clover Creek sequence	sanidine	11.67	0.02	14.7	2.6	14/25	CPT III	41.105498	-115.006608	This study

JC09-22	Tjrc	Jarbidge Rhyolite lava	Welcome, Clover Creek area	anorthoclase	15.35	0.04			27/27	M. Brueseke, personal commun. in McGrew and Snoke, 2015	41.0732	-115.0209	McGrew and Snoke, (2015)
H5EH-118	Th_1	Clover Creek	Welcome, Clover Creek area	anorthoclase	15.598	0.014	8.5	5.9	44/60		41.08834	-115.08176	This study
040731-1A	**Th_2**	reworked tephra in Ts	Humboldt Peak	sanidine	15.71	0.11	187	63.8	4/89	maximum depositional age; young population of 4 with similar age and K/Ca	40.9859	-115.052	This study
H21-W219	Tso_2	volcaniclastic deposit in Tso2	Welcome, Clover Creek area	sanidine	≤16.361	0.026	63.1		1/375	maximum depositional age; single youngest grain, consistent with U-Pb zircon youngest population	41.0825	-115.07629	This study
H21-W206A	Tso_2	calcite-cemented sandstone in Tso2	Welcome, Clover Creek area	sanidine	≤21.2			0.02	2/119	maximum depositional age; 2 youngest grains	41.08357	-115.0819	This study
H21-W174	Tso_2	volcanic sandstone in Tso2	Welcome, Clover Creek area	sanidine	≤22.9			0.06	2/31	maximum depositional age; 2 youngest grains	41.07601	-115.07721	This study
H21-W165	Tso_2	volcanic sandstone in Tmb	Welcome, Clover Creek area	sanidine	≤22.9			0.29	1/92	maximum depositional age; 1 youngest grain	41.07601	-115.07721	This study
8713-9	Tso_2	volcanic sandstone in Tmb	Welcome, Clover Creek area	sanidine	≤25.03					coherent group at 25 Ma	41.07485	-115.07893	This study
H21-W162	Tso_2	volcanic sandstone in Tmb	Welcome, Clover Creek area	sanidine	≤23.9			0.01	2/175	maximum depositional age; 2 young grains; 1 = 23.5	41.07485	-115.07893	This study
H21-W178C	Tso_2	volcanic sandstone in Tmb	Welcome, Clover Creek area	sanidine	≤22.08	0.17	68.2	20.4	13/166	maximum depositional age; distinct population of 13 youngest grains	41.06807	-115.07542	This study
H21-W178F	Tso_2	volcanic sandstone in Tmb	Welcome, Clover Creek area	sanidine	≤22.07	0.12	53.7	27.7	14/107	maximum depositional age; distinct population of 14 youngest grains	41.06807	-115.07542	This study
H10-79	Tvs	tuff of Campbell Creek	Welcome, Clover Creek area	sanidine	28.93	0.07	54.5	5.6	16/16		41.04326	-115.06825	Henry et al., (2012)
H21-W194	Tvs	cobble in conglomerate	Welcome, Clover Creek area	plagioclase	38.393	0.962	0.076	0.015	16/18		41.05209	-115.06673	This study
H18-47	outside map area	aft south of Spruce Mtn	south of Spruce Mtn	sanidine	38.232	0.0383	47.8	17.9	28/35		40.399223	-114.741891	This study
H11-9	Tbcc clast	tuff clast in sediments	Arizona Spring, south end of East	sanidine	39.77	0.26	115.4	97.4	9/11		40.69377	-115.07735	This study

			Humboldt Range										
H13-47	Tbcc	tuff of Big Cottonwood Canyon	Welcome, Clover Creek area	sanidine	40.21	0.02	74.0	18.5	8/20		41.07627	-115.09308	This study
H23-W288	Tbcc	not tuff of Big Cottonwood Canyon	Arizona Spring	sanidine	39.512	0.121	106.7	3.0	12/29	older population 40.076, 0.122, 71.2, 2.1, 15/29	40.68964	-115.08794	This study
H14-77	Th_2	Miocene tephra	Pequop Summit, Nanny Creek	sanidine	12.30	0.03	21.8	5.1	9/15		41.09474	-114.62503	This study
H14-78	Th_2	Miocene tephra	Pequop Summit, Nanny Creek	plagioclase	15.65	0.18	0.63	0.61	14/20		41.09283	-114.61868	This study
H15-39	outside map area	Miocene tephra	NW Pequop Mts	san/anorthoclase	15.18	0.04	11.3	5.1	13/16		41.18124	-114.67054	Zuza et al., (2019)
H17-32	outside map area	reworked tephra, upper gravel	Independence Valley NE	sanidine	≤1.97±0.78 or 3.99±0.23					very heterogeneous; 40.5-1.97 Ma, which is imprecise plag.	40.99053	-114.63470	Zuza et al., (2019)
H17-66	outside map area	sandstone	Independence Valley NE	sanidine	≤5.47	0.37	12.8	1	17/23	mean of group with same K/Ca	40.98078	-114.64449	Zuza et al., (2019)
H17-53	outside map area	tephra with steep dip	Independence Valley NE	sanidine	≤10.29	0.02	53	6.3	9/24	1 at, 8.09, 0.03	40.95686	-114.64283	Zuza et al., (2019)
WNC119-34	outside map area	tephra, lower gravel	Independence Valley NE	sanidine	≤8.80	0.27	plag		15/24	not very homogeneous plagioclase population; youngest = 6.69±0.11	40.96452	-114.64935	Zuza et al., (2019)
WNC119-77	outside map area	tephra, Agnico drillhole	Independence Valley NE	anorth	≤31.7	0.03	69.1	27.1	7/12	1 at ,12.88, 0.03	40.96452	-114.64935	Zuza et al., (2019)
WNC119-425	outside map area	tephra, Agnico drillhole	Independence Valley NE	sanidine	10.78	0.03	12.3	2.4	3/16		40.96452	-114.64935	Zuza et al., (2019)
WNC119-425R	outside map area	tephra, Agnico drillhole	Independence Valley NE	sanidine	≤10.72	0.01	14.3	2.2	3/16	coherent 3 in population with spread to 15.3 Ma	40.96452	-114.64935	Zuza et al., (2019)
H06-108	outside map area	tephra in sedimentary sequence above tuff of Big Cottonwood Canyon	Windermere Hills	sanidine	34.75	0.12	66.3	4.6	11/12		41.25438	-114.64428	This study
H11-9	outside map area, ash-flow	tuff clast in sediments	south end of East Humboldt Range	sanidine	39.77	0.26	115.4	97.4	9/11		40.69377	-115.07735	This study

	tuff clast in gravel												
H13-47	Tbcc	tuff of Big Cottonwood Canyon	Welcome	sanidine	40.21	0.02	74.0	18.5	8/20		41.07627	-115.09308	This study
H03-102	Tbcc	tuff of Big Cottonwood Canyon	Pequop Summit, Nanny Creek	sanidine	40.19	0.08	71.6	24.4	11/15		41.02779	-114.54667	This study
H03-103	Tx	tuff of Big Cottonwood Canyon	Pequop Summit, Nanny Creek	sanidine	40.34	0.1	73.8	37.6	13/15		41.02514	-114.52925	Henry (2008)
H05-38	Tbcc in Tx	tuff of Big Cottonwood Canyon	Pequop Summit, Nanny Creek megabreccia	sanidine	40.36	0.07	NA		14/15		41.03109	-114.52697	Henry (2008)
H03-111	outside map area	tuff of Big Cottonwood Canyon	Oxley Peak	sanidine	40.27	0.09	NA		15/15		41.19997	-114.91135	Henry (2008)
H03-101	Tpb	plagioclase-biotite tuff	Pequop Summit, Nanny Creek	plagioclase	40.95	0.13	0.1		18		41.02737	-114.54923	Henry (2008)

Table 2. Step heating $^{40}Ar/^{39}Ar$ analyses from volcanic metamorphic rocks in the Ruby Mountains–East Humboldt Range–Pequop Mountains map compilation, Nevada.

Sample	Map Unit	rock type	Location, quad	Material	Age data[1]											Notes	Latitude	Longitude	Source
					Plateau age (Ma)	±2s	%^{39}Ar[3]	n[2]	Isochron age (Ma)	±2s	^{40}Ar/^{36}Ari	±2s	MSWD	Total gas age (Ma)	±2s				
90B31B	Tvs	tuff of Big Cottonwood Canyon?	Welcome, Clover Creek area	biotite	≥38.5	0.5	54	9/12	NR					35.6	0.6	disturbed spectrum; no plateau	41.04712	-115.07028	Brooks, et al (1995a)
92BWH1	Qfo	rhyolite ash-flow tuff	Wood Hills	biotite	40.2	0.2	46.6	2/13	NR					40.49	0.18	weighted mean of disturbed spectrum	41.08132	-114.88278	Brooks et al (1995b)
91T10	Ta	dacite lava	Pequop Summit, Nanny Creek	hornblende	39.74	1	87	5/10	NR					39.9	0.3		41.02433	-114.54256	Brooks et al (1995a, b)
88T55	Qfi	tuff of Big Cottonwood Canyon	Pequop Summit, Nanny Creek	biotite	40.41	0.24	94	8/12	NR					40.16	0.26		41.02463	-114.53526	Brooks et al (1995a, b)
90B9B	Tbcc in Tx	tuff of Big Cottonwood Canyon	Pequop Summit, Nanny Creek	biotite	40.13	0.26	60	3/10	NR					39.9	0.4		41.02603	-114.53506	Brooks et al (1995a, b)
88T56	Qfi	plagioclase-biotite tuff	Pequop Summit, Nanny Creek	plagioclase	41.61	0.22	86	5/12	NR					41.59	0.26		41.02493	-114.53526	Brooks et al (1995a, b)
88T36	outside map area	probably tuff of Big Cottonwood Canyon	Oxley Peak	biotite	NM				NR					40	0.4		41.16575	-114.96255	Brooks et al (1995a, b)
88T38	outside map area	probably tuff of Big Cottonwood Canyon	Oxley Peak	biotite	40.37	0.3	95.9	10/12	NR					39.8	0.2	weighted mean of disturbed spectrum	41.16825	-114.95060	Brooks et al (1995a, b)

88T42	outside map area	dacite lava	Oxley Peak	biotite	40.2	0.2			NR					40.21	0.2	weighted mean of disturbed spectrum	41.20048	-114.91282	Brooks, et al (1995a)
88T41	outside map area	tuff of Big Cottonwood Canyon	Oxley Peak	biotite	40.28	0.26	63	6/13	NR					40	0.2		41.20103	-114.91088	Brooks et al (1995b)
WC-15	outside map area	ash-fall tuff	Windermere Hills	sanidine	35.24	0.36	31.4	2/13	NR					NR			41.25348	-114.64429	Mueller et al (1999)
WC-15	outside map area	ash-fall tuff	Windermere Hills	biotite	NM				NR					40.47	0.5	disturbed spectrum; no plateau	41.25348	-114.64429	Mueller et al (1999)
HOL-5	outside map area	rhyolite ash-flow tuff	Windermere Hills	sanidine	38.34	0.14	73.5	5/13	NR					NR		altered and does not fit stratigraphy, considered unreliable	41.24675	-114.62523	Mueller et al (1999)
HOL-4	outside map area	tuff of Big Cottonwood Canyon	Windermere Hills	sanidine	40.15	0.22	91	7/13	NR					NR			40.21129	-114.59761	Mueller et al (1999)
HOL-4	outside map area	tuff of Big Cottonwood Canyon	Windermere Hills	biotite	NM				NR					33.96	0.5		40.21129	-114.59761	Mueller et al (1999)
HOL-2	outside map area	andesite breccia	Holborn, eastern Windemere Hills	hornblende	39.688	0.24	92.8	5/13	NR					NR			41.24334	-114.63281	Mueller et al (1999)
WC-13	outside map area	rhyodacite lava flow	Wine Cup Ranch SW, eastern Windemere Hills	biotite	NM				NR					40.29	0.28	disturbed spectrum; no plateau	41.26609	-114.62731	Mueller et al (1999)
WC-6	outside map area	rhyodacite lava flow	Wine Cup Ranch SW, eastern Windemere Hills	hornblende	40.387	0.16	76.6	3/13	NR					NR			41.28984	-114.66579	Mueller et al (1999)
WC-1	outside map area	plag-biot tuff	Windermere Hills	biotite	40.9	0.12	63.8	4/13	NR								41.31436	-114.64254	Mueller et al (1999)
91T12	outside map area	dacite lava	Arizona Spring, southern East Humboldt Range	hornblende	39.3	0.8	71	5/13	NR					39.1	1.6		40.70303	-115.07368	Brooks et al (1995a, b)
91T17	outside map area	dacite lava	Arizona Spring, southern East Humboldt Range	hornblende	40.01	0.6	92	6/13	NR					40	0.8		40.66773	-115.10698	Brooks et al (1995a, b)
91T19	outside map area	dacite lava clast in conglomerate	Arizona Spring, southern East Humboldt Range	biotite	41.51	0.2	52.3	2/8	NR					39.98	0.32		40.69663	-115.07978	Brooks et al (1995a, b)
CLC-207	Oph	Lamprophyre dike	IVNE, Long Canyon	biotite	highly disturbed, probably Jurassic				127	9	1100	6000	10000	147	0.06		40.98353	-114.52426	This study
MRLC-1	O€np	Lamprophyre dike	IVNE, Long Canyon	biotite	highly disturbed, probably Jurassic				132	5	11000	700	200	138	0.08		40.96633	-114.53586	This study

H14-55	M€mu	mafic dike	Tent Mountain	matrix	17.01	0.06	50.3	4/13	16.85	0.1	301	3.5	1.9	17.67	0.03	40.88431	-115.23877	This study
H14-92	Tbl_2	basaltic andesite lava	Welcome	plagioclase	15.33	0.05	92.6	6/10	15.28	0.06	302.1	5	0.51	15.42	0.04	41.08933	-115.0534	This study
H14-107	Th_2	basaltic andesite clast in Th_2 (Boulder conglomerate)	Welcome	plagioclase	15.46	0.06	71.7	5/11	15.39	0.17	298.4	6.7	1.43	15.77	0.05	41.08963	-115.01308	This study
H14-65	Tbl_1	The Mound basalt	Tobar	plagioclase	17.63	0.96	81.6	4/13	16.68	0.08	859.7	44	1411	17.79	0.04	40.92935	-114.99362	This study
H14-66	Tbl_1	The Mound basalt	Tobar	matrix	16.92	0.04	60.1	6/13	17.06	0.06	276.8	7.6	5.74	16.99	0.01	40.92931	-114.99357	This study
H15-31	outside map area	basalt dike	Welcome, Angel Lake	plag matrix	excess Ar; no meaningful age				NM					467.2	1.1	41.02513	-115.08834	This study
H15-33	Tbd	basalt dike	Welcome, Angel Lake	matrix	excess Ar; no meaningful age				27.09	0.33	708.6	7.1	1080	62.9	0.6	41.02626	-115.08717	This study
H15-34	CZpm	basalt dike	Welcome, Angel Lake	plag	17.3	0.3	87.5	8/13	17	0.5	570	110	11	17.9	1	41.02343	-115.0877	This study
RM 643 A	outside map area	basalt dike	Harrison Pass area	whole rock	15.74	0.05								15.9	0.1	~40.346	~-115.540	Hudec (1990)
RM 643 B	outside map area	basalt dike	Harrison Pass area	whole rock	15.7	0.05								15.7	0.05	~40.346	~-115.540	Hudec (1990)
H13-48	Tvs	**tuff clast in sediments**		biotite	disturbed, climbing 33-37									34.67	0.17	41.04296	-115.07002	This study
H14-70	Ta	dacite lava	Pequop Summit, Nanny Creek	biotite	NM				NM					39.54	0.03	41.0351	-114.51882	This study
H14-89	Trd	rhyolite dike	Independence Valley NE	sericite	disturbed, 46-57 - 66				???							40.94335	-114.62989	This study
H14-88	€ks	muscovite leucogranite	Independence Valley NE	muscovite	NM				85.07	0.24				78.4	0.21	40.94271	-114.62947	This study
H14-123	Mc	Lamprophyre dike	Independence Valley SE	hornblende	161.5	0.24	74.8	3/7	158	3	1200	1000	14	160.3	0.088	40.84985	-114.61306	This study
H14-124	Mc	Lamprophyre dike	Independence Valley SE	hornblende	159.61	0.16	53.7	3/15	159.1	0.56	410	122	0.16	155.4	0.13	40.84985	-114.61306	This study
H14-64	Oph	Lamprophyre dike	IVNE, Long Canyon	hornblende	excess Ar				160.94	0.45	375	4	453	166.6	0.51	40.97249	-114.52764	This study
H09-93B	O€np	Lamprophyre dike	IVNE, Long Canyon	hornblende	excess Ar				165	2	4.9	1039	186	209	1	40.97155	-114.52757	This study
DV-9-16-21 (4)	Mdp	lamprophyre dike	Independence Valley SE	hornblende	161.49	0.86	78	10/18	161.7	1.19	291.73	27.2	1.53	156.87	0.88	40.80758	-114.61829	This study

[1] $^{40}Ar/^{39}Ar$ analyses of this study were done at the New Mexico Geochronological Research Laboratory (methodology in McIntosh et al., 2003; Henry et al., 2017). Neutron flux monitor Fish Canyon Tuff sanidine (FC-1) with assigned age = 28.201 Ma (Kuiper et al., 2008).

Published ages of Brooks et al. (1995a, b) were recalculated to the same monitor age.

Decay constants after Min et al. (2000); ltotal = 5.463 x 10-10 yr-1. Isotopic abundances after Steiger and Jäger (1977); 40K/K = 1.167 x 10-4

NM = not meaningful; no plateau. NR = not reported.

[2] n = number of steps used in age calculation/total number of analytical steps.

[3] %^{39}Ar = percentage of ^{39}Ar used to define plateau age.

Dates in bold are best estimates of eruption or emplacement age.

Table 3. Summary of zircon U-Pb ages of plutonic rocks in the Ruby Mountains– East Humboldt Range– Pequop Mountains map compilation, Nevada.

Sample	Map unit	Rock type	Location	n	U-Pb age* (Ma)	± 1s (Ma)	MSWD	Latitude	Longitude	Reference
Ruby Mountains-East Humboldt Range										
AZ8-19-19(6)	Tmg	monzogranite	western East Humboldt Range	21	31.3	0.2	1.10	40.95752	-115.20163	Zuza et al. (2022)
AZ7-28-20(4)	Tmg	monzogranite	western East Humboldt Range	29	32.5	0.3	1.60	40.990739	-115.12566	Zuza et al. (2022)
060720-4	Tmg	quartz diorite	western East Humboldt Range	67	39.9	0.2	1.90	40.950218	-115.22081	Zuza et al. (2022)
AZ 6-30-20 (6)	OꞒm	quartz diorite	western East Humboldt Range	34	38.7	0.3	1.60	40.954877	-115.222	Zuza et al. (2022)
AZ 6-8-21 (1)	TKlg	leucogranite	Dorsey Creek	7	36.8	1	0.30	40.8806	-115.22516	Zuza and Dee (2023)
AZ 9-18-21 (1)	Tgd	granodiorite	Dorsey Creek	22	39.1	1.2	0.61	40.87587	-115.24463	Zuza and Dee (2023)
AZ 6-6-21 (1)	Tgo	granitic orthogneiss	western East Humboldt Range	20	38.9	1.2	0.87	40.91322	-115.22119	Zuza and Dee (2023)
AZ 7-15-21 (3)	Tmg	granitic orthogneiss	northern Ruby Mountains	20	30.9	0.9	0.93	40.82692	-115.25543	Zuza and Dee (2023)
AZ 8-18-22 (1)	Tvs	andesite	southern East Humboldt Range	13	40.1	0.4	1.50	40.70057	-115.07090	This study
AZ 7-28-22 (3)	Tmg	monzogranite	Angel Lake	26	32.1	0.2	8.90	41.03078	-115.09311	This study
H21-W162	Tso_2	volcanic sandstone, detrital	Clover Creek	132	≤21.0	0.7	NM	41.07485	-115.07893	This study
H21-W174	Tso_3	volcanic sandstone, detrital	Clover Creek	102	≤21.1	0.6	NM	41.07601	-115.07721	This study
H21-W178	Tso_2	volcanic sandstone, detrital	Clover Creek	108	≤21.4	0.5	NM	41.06807	-115.07542	This study
H21-W219	Tso_3	volcanic sandstone, detrital	Clover Creek	107	≤16.6	0.2	3.40	41.08250	-115.07629	This study
AZ 10-20-20 (1)	OꞒm	quartzite, detrital	western East Humboldt Range	200	NM	NM	NM	40.941456	-115.22479	Zuza et al. (2022)
HR 12-03	Oe	quartzite, detrital	Angel Lake	168	NM	NM	NM	41.025861	-115.09167	Zuza et al. (2022)
AZ 10-21-20 (5)	OꞒm	quartzite, detrital	western East Humboldt Range	182	NM	NM	NM	40.98838	-115.105	Zuza et al. (2022)
AZ 10-21-20 (11)	MꞒmu	quartzite, detra	western East Humboldt Range	29	NM	NM	NM	40.99079	-115.112	Zuza et al. (2022)
AZ 10-8-19 (1a)	Mdp	fine-grained mylonite, detrital	Secret Valley	86	NM	NM	NM	40.83177	-115.14803	Zuza et al. (2022)
AZ 7-27-22 (3)	CZpm	quartzite	Clover Hill	115	NM	NM	NM	41.044754	-115.00866	This study
AZ 8-18-22 (7)	Zmum	quartzite	southern East Humboldt Range	249	NM	NM	NM	40.869222	-115.068133	This study
Pequop Mountains										
PQSG	Opks	gabbro	Central high part of range	2	159.0	6.0	NR	40.94167	-114.57885	Bedell et al. (2010)
34FGG	Ꞓs	foliated aplite-rhyolite dike	West Pequop	14	159.5	1.9	NR	40.96345	-114.60484	Bedell et al. (2010)
SWPQR1	Trd	rhyolite dike	Southwest Pequops	6	41.0	0.8	NR	40.92990	-114.64268	Bedell et al. (2010)
SWPQR2	Ꞓks	rhyolite dike	Southwest Pequops	12	39.1	0.7	NR	40.94330	-114.62960	Bedell et al. (2010)
SWCGG	Ꞓt	leucogranite dike	Southwest Pequops	2	71.0	5.0	NR	40.93960	-114.63240	Bedell et al. (2010)
Rockland	ℙe	granodiorite; porphyritic	Southern Pequops		161.4	1.9	NR	40.79140	-114.61940	Bedell et al. (2010)
DV-9-16-21(6)	Mdp	Lamprophyre	Southern Pequops	14	160.7	2.8	2.8	40.80543	-114.62185	Vlaha and Zuza (2022)

DV-9-17-21(6)	Mdp	granite	Southern Pequops	9	161.7	0.5	0.45	40.79310	-114.61510	Vlaha and Zuza (2022)
H14-82	Ꞓcl	granite	Meyers Canyon	13	155.6	0.8	1.4	40.99429082	-114.612759	Zuza et al. (2021)
PFW1	Oe	quartzite, detrital	central Pequops	139	NM	NM	NM	40.97812	-114.57	Zuza et al. (2022)

*Often $^{206}Pb/^{238}U$ age for igneous samples; maximum depositional age for detrital analyses
NM: not meaningful; NR: not reported